ATTACHMENT B: AREA OF REVIEW AND CORRECTIVE ACTION PLAN

Facility Information

Facility name: Kansas Small Scale Test Wellington Field
KSS191GS0001

Facility contact: Dana Wreath, Vice President – Berexco LLC
2020 North Bramblewood Dr., Wichita, KS, 67206
Tel: (316) 337-8331
Fax: (316) 265-8690

Well location: Sumner County, KS
Latitude 37.319485, Longitude -97.4334588

Computational Modeling Approach

Model Background

The computational model used for this effort is the Computer Modeling Group (CMG) GEM simulator. GEM is a full equation of state compositional reservoir simulator with advanced features for modeling the flow of three-phase, multi-component fluids and has been used to conduct numerous CO_2 studies.[1,2] It is considered by DOE to be an industry standard for oil/gas and CO_2 geologic storage applications. The code can account for the thermodynamic interactions between three phases: liquid, gas, and solid (for salt precipitates). Mutual solubilities and physical properties can be dynamic variables depending on the phase composition/system state and are subject to well-established constitutive relationships that are a function of the system state (pressures, saturation, concentrations, temperatures, etc.). The following equations and assumptions govern the phase interactions:

- Gas solubility obeys Henry's Law.[3]
- The fluid phase is calculated using Schmit-Wenzel or Peng-Robinson (SW-PR) equations of state.[4]

[1] Chang, K. W., Minkoff, S. E., and Bryant, S. L., 2009, Simplified model for CO2 leakage and its attenuation due to geological structures: Energy Procedia, v. 1, p. 3,453–3460.

[2] Bui, L. H., Tsau, J. S., and Willhite, G. P., 2010, Laboratory investigations of CO2 near-miscible application in Arbuckle Reservoir: SPE Improved Oil Recovery Symposium held in Tulsa, Oklahoma, 24–28 April 2010. SPE Publication 129710.

[3] Li, Y. K., and Nghiem, L. X., 1986, Phase equilibrium of oil, gas and water/brine mixtures from a cubic equation of state and Henry's Law: Canadian Journal of Chemical Engineering, June, p. 486–496.

[4] Soreide, I., and Whitson, C. H., 1992, Peng-Robinson predictions for hydrocarbons, CO2, N2, and H2S with pure water and NaCl brine: Fluid Phase Equilibria, Vol. 77, p. 217-240.

- Changes in aqueous phase density with CO_2 solubility, mineral precipitations, etc., are accounted for with the standard or Rowe and Chou correlations.
- Aqueous phase viscosity is calculated based on Kestin, Khalifa, and Correia (1981).[5]

Ambient pore pressure, temperature, and salinity vary nearly linearly with depth in the Arbuckle Group. By linear extrapolation, the relationship between depth and these three parameters can be expressed by the following equations, where depth is in feet below Kelly Bushing (KB):

- Temperature (°F) = (0.011 * Depth + 73.25)
- Pressure (psi) = (0.487 * Depth – 324.8)
- Chloride (mg/l) = (100.9 * Depth – 394.786)

A uniform salinity concentration was assumed, as the effects of water salinity on the simulated AoR were found to be negligible (less than 5%). The ambient reservoir temperature of 140 ^{o}F was assumed for the entire model domain, considering the injection zone is narrow and the temperature gradient is not significant enough to affect the petrophysical properties. Multiple physical processes were modeled in the reservoir simulation to account for multiple states, physiochemical conditions, and temporal changes. The physical processes accounted for in the reservoir simulations are multi-phase flow and transport of brine and CO_2, with specific processes including: advection, dispersion, diffusion, buoyancy, non-wetting fluid trapping, pore compressibility, heat transport. Processes of structural trapping, aqueous dissolution, and hydraulic trapping were simulated in the Wellington model, while geochemistry (mineral trapping) and structural deformations were not modeled. It was unnecessary to model pore velocity (groundwater velocity); assuming an average large-scale Arbuckle porosity of approximately 6% and a median permeability of 10 mD, the pore velocity in the Arbuckle is approximately 0.2 feet/year and can therefore be neglected in the specification of ambient boundary conditions for this modeling study. In terms of multi-fluid flow processes, dispersion and diffusion processes were not modeled since the inclusion of these calculations in the full-scale dynamic simulation required significantly more processing time. Sensitivity runs were performed with dispersion and diffusion to demonstrate the impact of these parameters.

Geochemical reactions are not considered in this modeling effort due to the low probability and low risk of high impacts within the Arbuckle system. Mineralization as a trapping mechanism was not simulated, as geochemical modeling indicated that, due to the short-term and small scale nature of this project, mineral precipitation is not expected to cause any problems with clogging of pore space that may reduce permeability and negatively impact injectivity. If carbonate precipitation and other forms of geochemical trapping are expected to occur to any significant degree, the permittee will model them as part of the AoR re-evaluation at the end of the injection period, using injection phase data to update the model, to support the non-endangerment demonstration.

[5] Kestin, J., Khalifa, H. E., and Correia, R. J., 1981, Tables of the dynamic and kinematic viscosity of aqueous NaCl solutions in the temperature range 20–150 °C and the pressure range 0.1–35 MPa: Journal of Physical and Chemical Reference Data, NIST, v. 10, p. 71–88.

Processes were modeled under isothermal conditions because the temperature of the injected CO_2 will equilibrate to original reservoir temperature fairly quickly and the lateral extent of the temperature drop was limited around the wellbore, which should not significantly affect the various storage modes away from the injection well. Furthermore, non-isothermal sensitivity simulations were conducted as described later in this plan.

Site Geology and Hydrology

Note: The following sections summarize the regional and local geological and hydrological conditions at the Wellington Site. This information, which serves as inputs for the AoR delineation modeling, is based on information in the permit application and subsequent submittals from Berexco. For additional information documenting EPA's evaluation of regional and local site characterization, please see the report, "Geologic Data for Site Characterization at the Berexco-Kansas Small Scale Test Wellington Field: EPA Evaluation, Analysis, and Conclusions."

This Class VI project has an injection depth between 4,910 and 5,050 feet in the lower portion of the regionally-extensive Arbuckle formation. The primary confining zone at the injection site comprises the overlying Simpson Group, Chattanooga Shale, and the Pierson Formation in the interval 3,930 – 4,168 feet. There are several additional shale layers between the injection zone and the base of the Upper Wellington Formation that can provide secondary hydraulic confinement, although that was not considered for the purpose of this modeling effort.

REGIONAL GEOLOGY:

Injection will occur in the lower portion of the Cambrian/Ordovician-age Arbuckle Group, which is a large saline aquifer present throughout the midcontinent region of the United States. It lies above the Precambrian-age granitic basement, which is also prevalent throughout Kansas and is expected to provide impediment to flow, functioning as the lower confining zone for the project. The presence and regional continuity of the injection zone is demonstrated by structure maps and stratigraphic columns. In Sumner County (the location of this project), the Arbuckle Group is approximately 1,000 feet thick and includes several shaley intervals ranging in thickness from 50 to 425 feet as described later in this plan. The Arbuckle aquifer in southern Kansas is suitable as an injection zone from the perspective of salinity, given that total dissolved solids (TDS) levels are too high in the Arbuckle aquifer for it to qualify as a USDW; at the Wellington test site, Arbuckle brines had TDS values ranging from ~48,000 mg/L in the Upper Arbuckle (at 4,182 feet) to 180,000 mg/L in the Lower Arbuckle (at 5,005 feet) as determined from drill stem tests (DST) and swab tests.

The injection zone is vertically segregated from the Upper Wellington Formation in the region by multiple shale formations. The upper confining zone is defined as rock units from the base of the Simpson Group through the top of the Pierson Formation, including the Chattanooga Shale. Units in the lower portion of the confining zone are composed primarily of shaley limestone and shale, while confining units overlying those are primarily shale with varying amounts of sandstone.

There is a regionally extensive fault zone located approximately 12 miles east of the injection site. The fault zone is mapped on the top surface of the Precambrian granites parallel to the Nemaha Uplift, a ridge that plunges to the south and consists of granitic basement rock that predates the deposition of the Arbuckle Group. Tectonic activity occurred along the fault zone during the late Mississippian and early Pennsylvanian during a period of growth of the Nemaha Uplift[6] (Dolton and Finn, 1989).

LOCAL GEOLOGY:

Site-specific data used to characterize the local hydrogeologic properties of the injection and confining zone are shown in Table 1. Field data were collected at KGS 1-28 (injection well) and KGS 1-32 (geologic test well), including well logs and some core samples. Seismic data were collected at the Wellington site. Baseline geochemical data were collected in the Mississippian, Arbuckle, and Precambrian basement, and will be used to track the CO_2 plume evolution during and after injection.

Based on geophysical logs in KGS 1-28, the upper confining zone is present from 3,930 – 4,168 feet. The top of the Arbuckle injection formation in the Wellington area is at a depth of approximately 4,170 feet, which is well below the 2,500+ feet required for maintaining CO_2 in the supercritical state. The Arbuckle extends from approximately 4,170 feet to 5,160 feet. The logs confirm the presence of the granitic basement, the Arbuckle Group, the confining zone, and the Mississippian System at approximately the same elevation at both sites.

The core samples, along with geophysical logs, geochemical information, laboratory-based permeability estimates, and seismic data, all indicate the presence of three distinct hydrogeologic zones within the Arbuckle: a tight (low impedance) baffle zone in the middle and relatively more permeable zones above and below the baffle zone. These distinct hydrogeologic zones correspond to the lithological heterogeneity in the Arbuckle Group.

The mid-Arbuckle baffle zone consists of tight, dense, micritic dolomite and contains multiple low-permeability intervals. Extensive pore-space silicification and infilling by argillaceous material has been observed in thin section and could be a major factor controlling porosity reduction in the baffle zone. The potential of a geologic baffle, or low-permeability zone, within the Arbuckle has important implications for the movement of the injected CO_2. As the CO_2 plume migrates vertically, it could be trapped within or under the baffle.

Based on the results of DSTs, the Mississippian system, which includes the top of the upper confining interval as well as more porous formations above, is highly under-pressurized relative to the Arbuckle, further supporting the hypothesis of hydrologic separation of the Mississippian and Arbuckle rock units.

[6] Dolton, G., and Finn, T., 1989. Petroleum Geology of the Nemaha Uplift, Central Mid-Continent. USGS Open-File Report 88-450D.

Table 1. Data collected as part of well testing and logging, and location in the permit application.

Acquired Data	Section of Application where Documented/Discussed
Geophysical Logs	
Array Compensated True Resistivity	Appendices B and C, Section 4.4
Temperature	Appendices B and C, Section 4.6.5
Compensated Spectral Gamma Ray	Appendices B and C, Sections 4.6 and 4.7
Microlog	Appendices B and C
Spectral Density Dual Spaced Neutron Log	Appendices B and C, Sections 4.6 and 4.7
Annular Hole Volume Log	Appendices B and C
Extended Range Micro Imager Correlation Plot	Appendices B and C, Section 4.7
Magnetic Resonance Image Log	Appendices B and C, Sections 4.6 and 4.7
Radial Cement Bond Log	Appendices B and C
CT Scan	Section 4.7.5.3
Core Samples (Arbuckle Group)	
Porosity and Permeability	Section 4.6.6
Mineralogy and Soil Characterization	Section 4.6.2
CO_2 Compatibility	Section 4.6.10
Drill-Stem Test	Sections 4.6.3 and 8.15.3
Geochemistry	Section 4.6.7
Pressure and Temperature	Sections 4.6.3 and 4.6.5
Swab Samples	
Geochemistry	Section 4.6.7
Injection Test	
Permeability	Section 4.6.4
Seismic Data	
Structure and Impedance Mapping	Section 4.8
Core Samples (Confining Zone)	
Porosity and Permeability	Section 4.7.3
Mineralogy and Soil Characterization	Section 4.7.2
CO_2 Compatibility	Section 4.7.7
Fracture Studies	Section 4.7.5.1

A pulse test was conducted at KGS 1-32 to estimate transmissivity and hydraulic conductivity of the injection interval. Results yielded a reasonably good match between the observed and modeled response at KGS 1-32, with a permeability value of 250mD. The highly-varying permeability and porosity values determined from log and core data were extrapolated to the entire reservoir using Schlumberger's Petrel geo-cellular software. A continuous vertical porosity profile was derived using NMR logs. Porosity is variable throughout the Arbuckle Group and exists due to small, isolated intercrystalline to large vuggy openings. The core-based estimates of porosity vary widely (0.3 – 27.3%) with an average value of 3.4%. The porosity is highest in the upper and lower portions of the Arbuckle, and there is relatively lower porosity in the middle Arbuckle baffle zone.

In the original permit application, Berexco identified the Upper Wellington Formation as the lowermost USDW based on regional data and injection site estimates of TDS. However, further investigation of site-specific data and additional sampling in October 2015 led to a determination that the Upper Wellington formation does not meet the criteria to be classified as a USDW in the project area. For additional information on EPA's determination that no USDW exists within the AoR, see the document, *EPA Determination Regarding the Presence of a USDW within the AoR at the Wellington Site*.

The major sealing units immediately above the Arbuckle injection zone are comprised of shales and argillaceous siltstone within the Simpson Group, the Chattanooga Shale, and the Pierson Formation as shown in Figure 1 below.

The confining zone is laterally continuous at the Wellington storage site as identified by well logs from KGS 1-28, 1-32, and 2-28. In addition to the log analyses and results of laboratory-based estimates of permeability and porosity, the sealing potential of the confining zone can also be estimated from the pore entry pressure, defined as the capillary pressure at which the non-wetting phase enters the largest pores. Entry pressure in the confining zone was calculated at KGS 1-32 and 1-28 using the Techlog wellbore software platform. The maximum entry pressure at KGS 1-28 was 956 psi. As discussed later in this Plan, the maximum induced CO_2 pressure at the top of the Arbuckle/base of the Simpson is approximately 13.1 psi. Therefore, the likelihood of the injected CO_2 escaping through or compromising the confining zone is negligible.

Core-based fracture studies, XMRI log-based fracture investigations, and CT scan analysis were conducted at the injection site to determine the presence or absence of fractures in the confining zone. Continuous core was cut at KGS 1-32 between the depths of 3,540 and 5,179 feet for the core-based fracture studies. Most of the fractures identified are completely occluded by mineralization (quartz, dolomite, and calcite). Although there are many fractures in the Simpson Group, these are mainly confined to chert nodules, which are the consequence of diagenesis. These fractures do not negatively affect the sealing nature of the confining zones[7]. Also, almost all of the fractures within the Simpson Group are in the sands and dolomite and not in the shaley intervals, which provide the hydraulic confinement.

[7] Watney, W.L., Guy, W.J., and Byrnes, A.P., 2001, Characterization of the Mississippian Osage Chat in South-Central Kansas: American Association of Petroleum Geologists Bulletin, v. 85, p. 85-114.

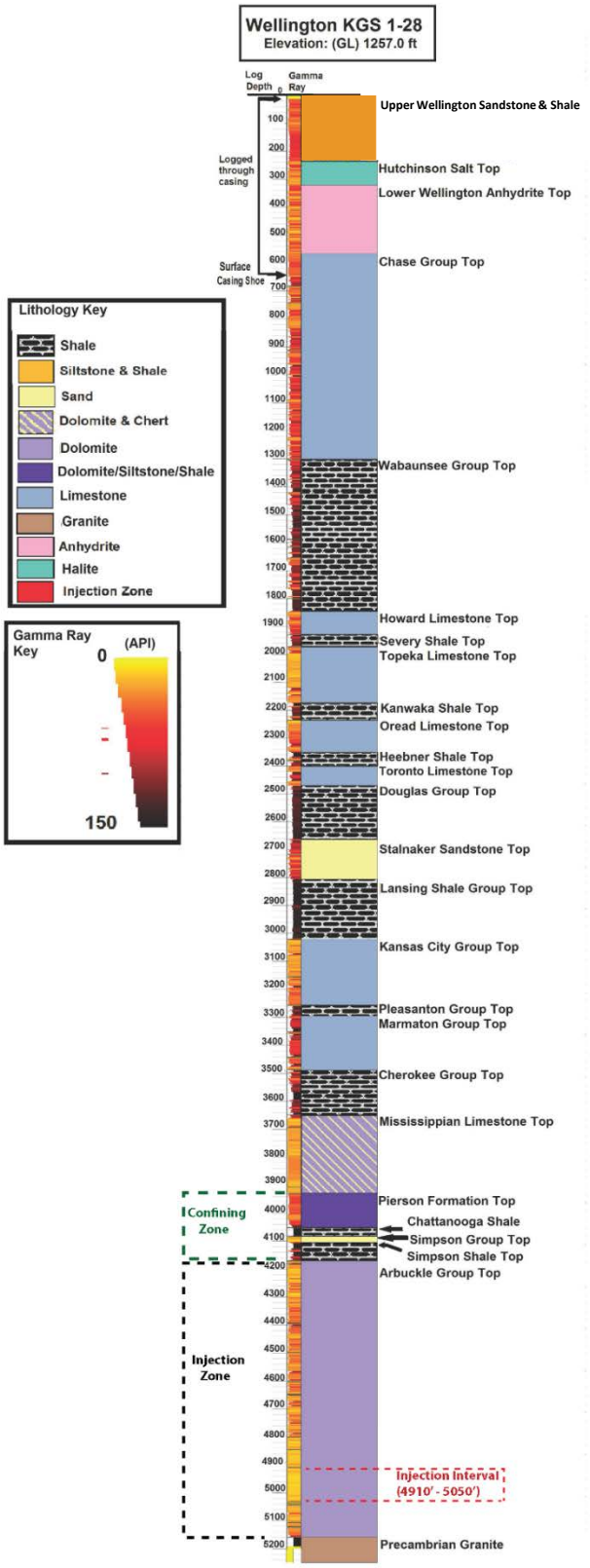

Figure 1. Stratigraphic column at the KGS 1-28 well.

Model Domain

Model domain information is summarized in Table 2. The modeled area is centered approximately on the injection well, and extends 1.3 mi by 1.2 mi laterally, with a vertical thickness of approximately 1,000 feet. This model area has a total surface area of roughly 1.56 mi^2 and a total volume of approximately 0.2955 mi^3. Simulation occurred over the entire thickness of the Arbuckle aquifer, with no-flow boundaries defined at the top and bottom of the model (i.e., the model does not include the confining zone and the Precambrian basement). Details on these boundary conditions are included later in this Plan.

Table 2. Model domain information.

Coordinate System	State Plane		
Horizontal Datum	Other		
Coordinate System Units	Feet		
Zone	Kansas SPCS27-1502		
FIPSZONE	1502	**ADSZONE**	3926
Coordinate of X min	2,305,362	**Coordinate of X max**	2,313,727
Coordinate of Y min	235,940	**Coordinate of Y max**	243,907
Elevation of bottom of domain (ft)	3893	**Elevation of top of domain**	2814

The original geomodel mesh was generated using the Petrel geomodel. The total size was 706 x 657 x 79 (x, y, z) for a total of 36,476,196 cells from the base of the Arbuckle Group to the top of the Pierson Group. This grid size is computationally intensive and inefficient, so the original mesh was upscaled to reduce reservoir simulation time. The upscaled model mesh, shown in Figure 2 and Figure 3, is 157 x 145 x 79 for a total of 1,798,435 cells. Grid scaling is variable depending on the location within the Arbuckle, but is consistent laterally away from the injection well. The tightest grid cells are present in the injection interval (4,910 – 5,050 feet); relatively tight grid spacing was selected in the top 200 feet of the Arbuckle (near the base of the confining zone) and in the 100 feet immediately above the perforated zone; the loosest grid spacing was defined in the mid-Arbuckle baffle zone (between ~4,300 and 4,700 feet) and immediately above the Precambrian basement rock. In the upscaled model mesh, the layer thickness varies from 5 to 20 feet based on the thickness in the original Petrel geomodel (average = 13 feet).

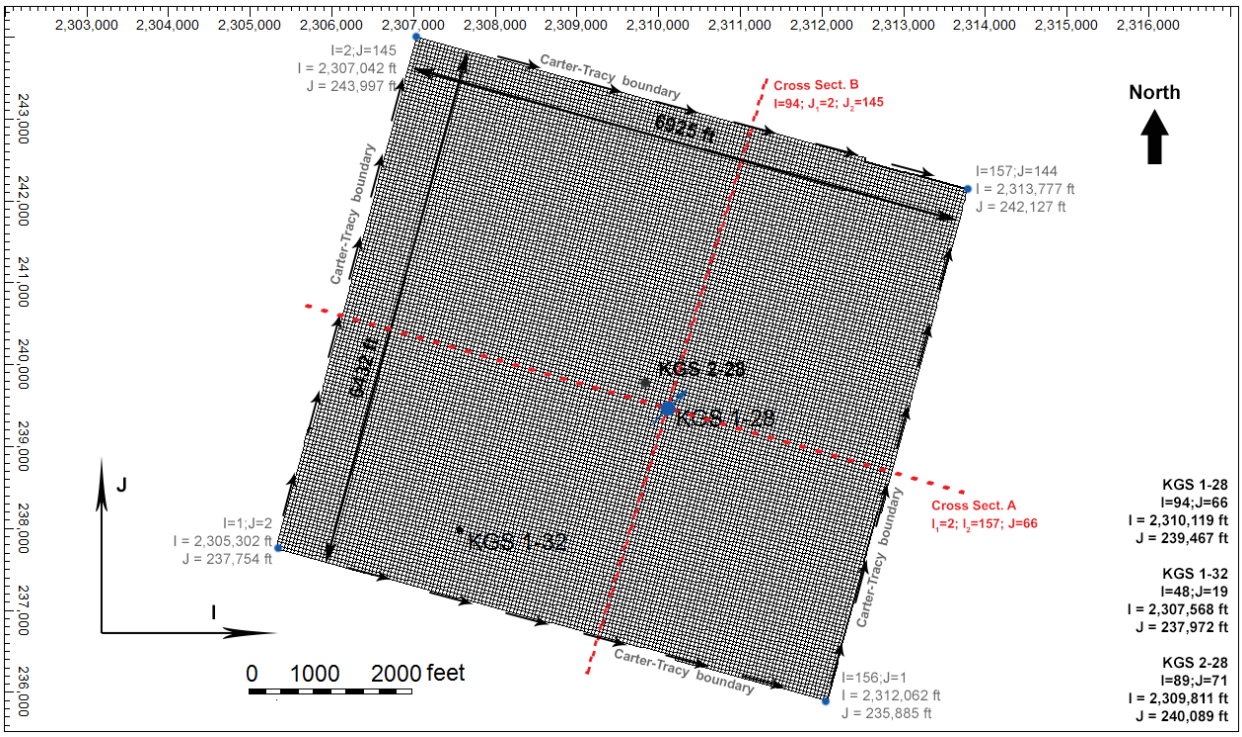

Figure 2. Plan-view image showing the upscaled model grid with model coordinates. Red hashed lines represent the cross sections presented in Figure 3 and other figures in this plan.

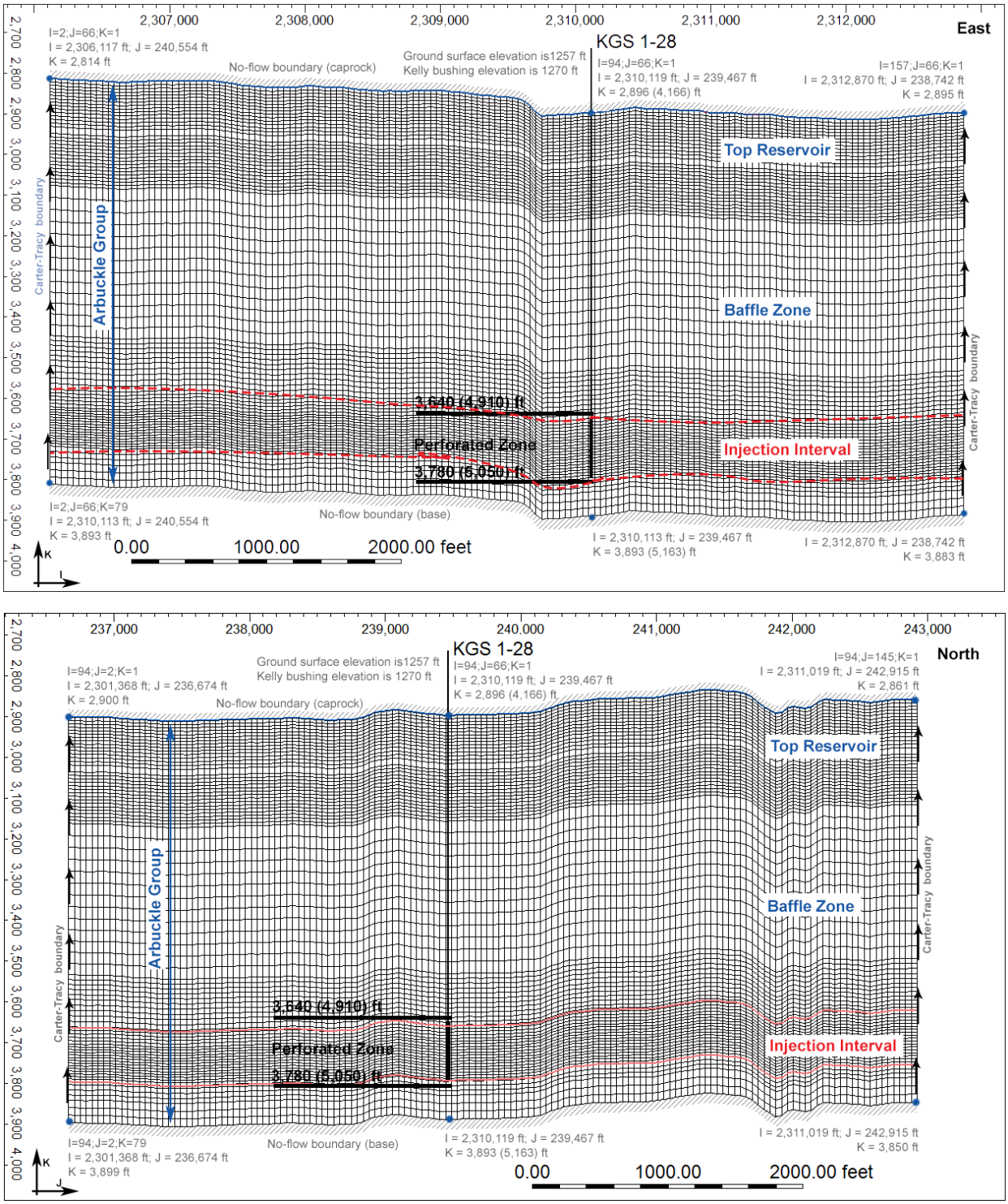

Figure 3. Cross-sections showing the E-W (top) and N-S (bottom) distribution of grid cells in the upscaled model mesh.

Porosity and Permeability

Porosity and permeability were modeled using Schlumberger's Petrel geologic model using the data and methods described below. The geomodel extends 1.3mi by 1.2mi laterally and is approximately 1,000 feet thick, spanning the entire Arbuckle Group as well as a portion of the sealing units (Simpson/Chattanooga shale), as described in more detail earlier in this Plan. Core samples were used to reconcile variations between whole core, step-rate tests, and permeability measurements from wireline logs. There was generally poor core recovery due to vuggy rocks.

Wireline logs in KGS 1-28 and 1-32 and seismic data provide information on facies and porosity trends within the geomodel. In addition to the well log data, the geologic model also relied on seismic data, step-rate test results, and drill-stem test information. Core samples were not obtained at KGS 1-28 (injection well), and therefore the horizontal permeability was estimated at this site using the methodology of Fazal Alavi et al. (2013).[8] The volume attribute processing (i.e., genetic inversion) capability of Petrel was used to derive a porosity attribute from the prestack depth migration (PSDM) volume to generate the porosity model. The seismic volume was created by re-sampling (using the original exact amplitude values) the PSDM 50 feet above the Arbuckle and 500 feet below the Arbuckle (approximate basement depth). The cropped PSDM volume and conditioned porosity logs were used as learning inputs during neural network processing.

A correlation threshold of 0.85 was selected and 10,000 iterations were run to provide the best correlation for modeling porosity distributions. The resulting porosity attribute was then re-sampled, or upscaled (by averaging), into the corresponding 3D property grid cell. The porosity distribution model was then constructed using sequential Gaussian simulation (SGS). Figure 4 and Figure 5 show the porosity distribution in 3D and cross-sections respectively.

[8] Fazel Alavi, M., Fazel Alavi, M., and Fazel Alavi, M., 2013, Determination of reservoir permeability based on irreducible water saturation and porosity from log data and FZI (flow zone indicator) from core data, International Petroleum Technology Conference in Doha, Qatar, IPTC-17429-MS, Richardson, TX.

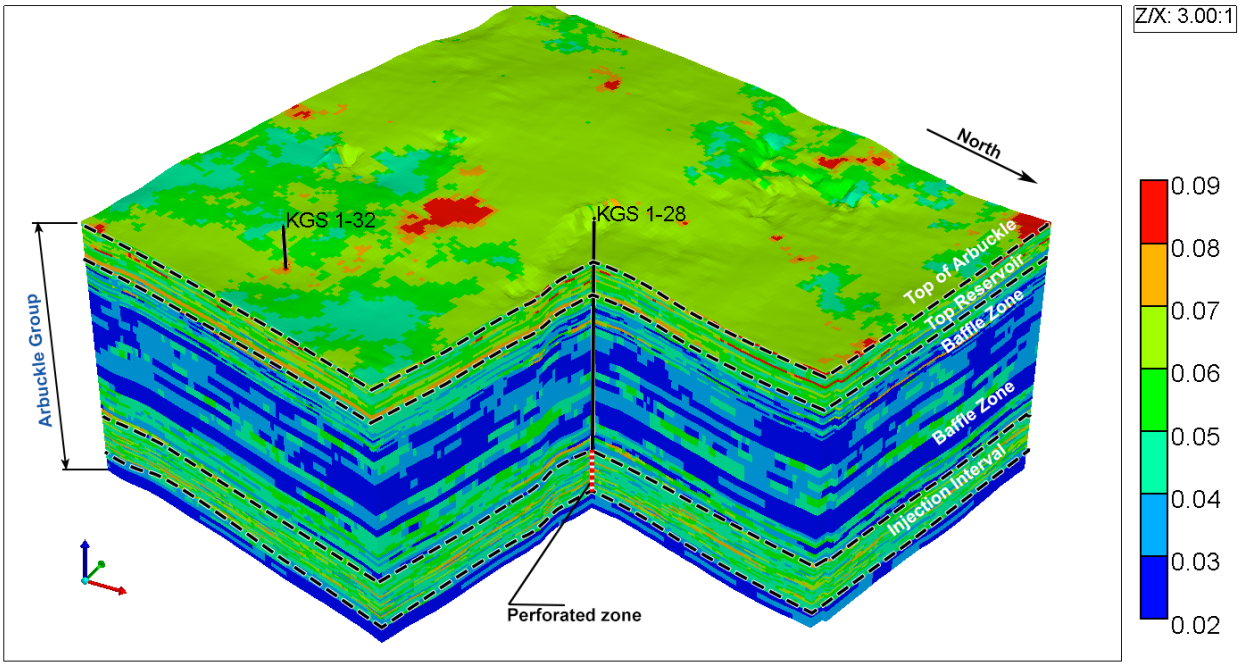

Figure 4. Upscaled porosity distribution in the Arbuckle Group based on the results of the Petrel geomodel.

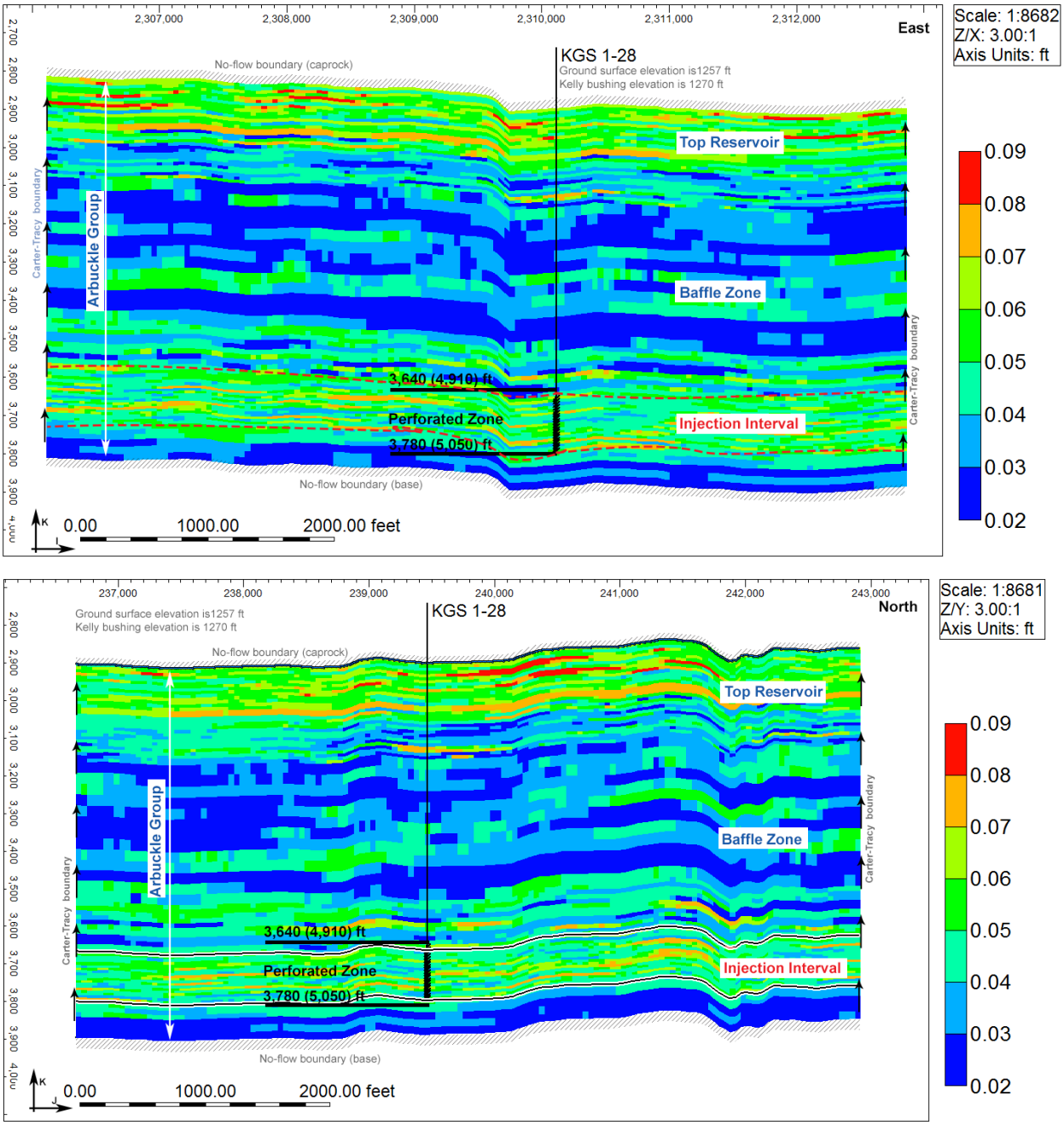

Figure 5. Cross-sections of the upscaled porosity distribution in the E-W (top) and N-S (bottom) orientations. The locations of the cross sections are shown in Figure 2.

The upscaled permeability logs were created using the following controls: geometric averaging method; logs were treated as points; and method was set to simple. The permeability model was constructed using SGS. The permeability was collocated and co-kriged to the porosity model using the calculated correlation coefficient (~0.70). The vertical permeability in most of the confining zone is less than 0.005 mD, derived from core-based estimates. In general, the horizontal permeability in the Pierson and Chattanooga Shale (upper portions of confining zone) is very low. In the Simpson Group (lower portion of confining zone), the permeability is higher in the sand intervals and much lower in the shale zones. Figure 6 and Figure 7 show the horizontal permeability distribution for the model grid in 3D and cross-sections respectively. Figure 8 presents the vertical permeability distribution for each cross-section. Statistics related to the reservoir geophysical properties modeling are presented in Table 3 below.

Table 3. Rock property statistics for the reservoir characterization models.

	Reservoir Characterization Geomodel			Reservoir Simulation Numerical Model		
Property	Min	Max	Mean	Min	Max	Mean
Porosity (%)	3.2	12.9	6.8	3.2	12.9	6.7
Horizontal Permeability (mD)	0.05	23,765	134.2	0.05	23,765	130.7
Vertical Permeability (mD)	0.005	58,168	387	0.005	58,168	385

Information on incorporating the results of pre-injection testing and monitoring into AoR reevaluations, and using data as triggers for unscheduled reevaluations, is described later in this Plan.

Horizontal Permeability Images:

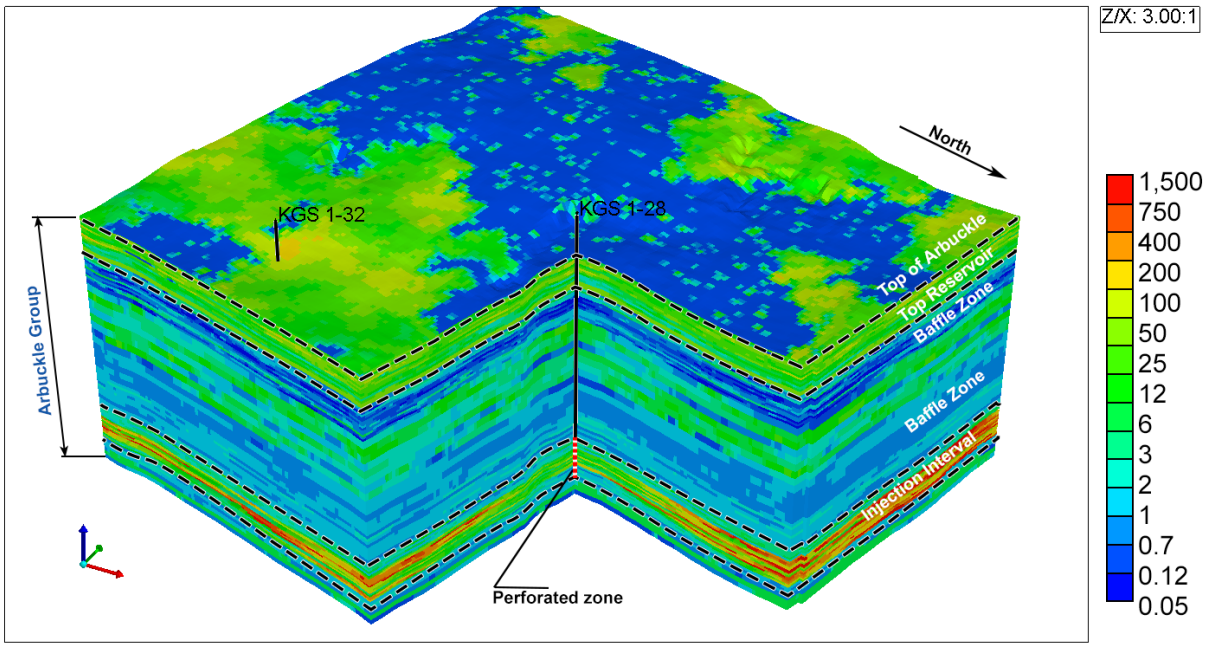

Figure 6. Upscaled horizontal permeability (mD) distributions in the Arbuckle Group derived from the Petrel geomodel.

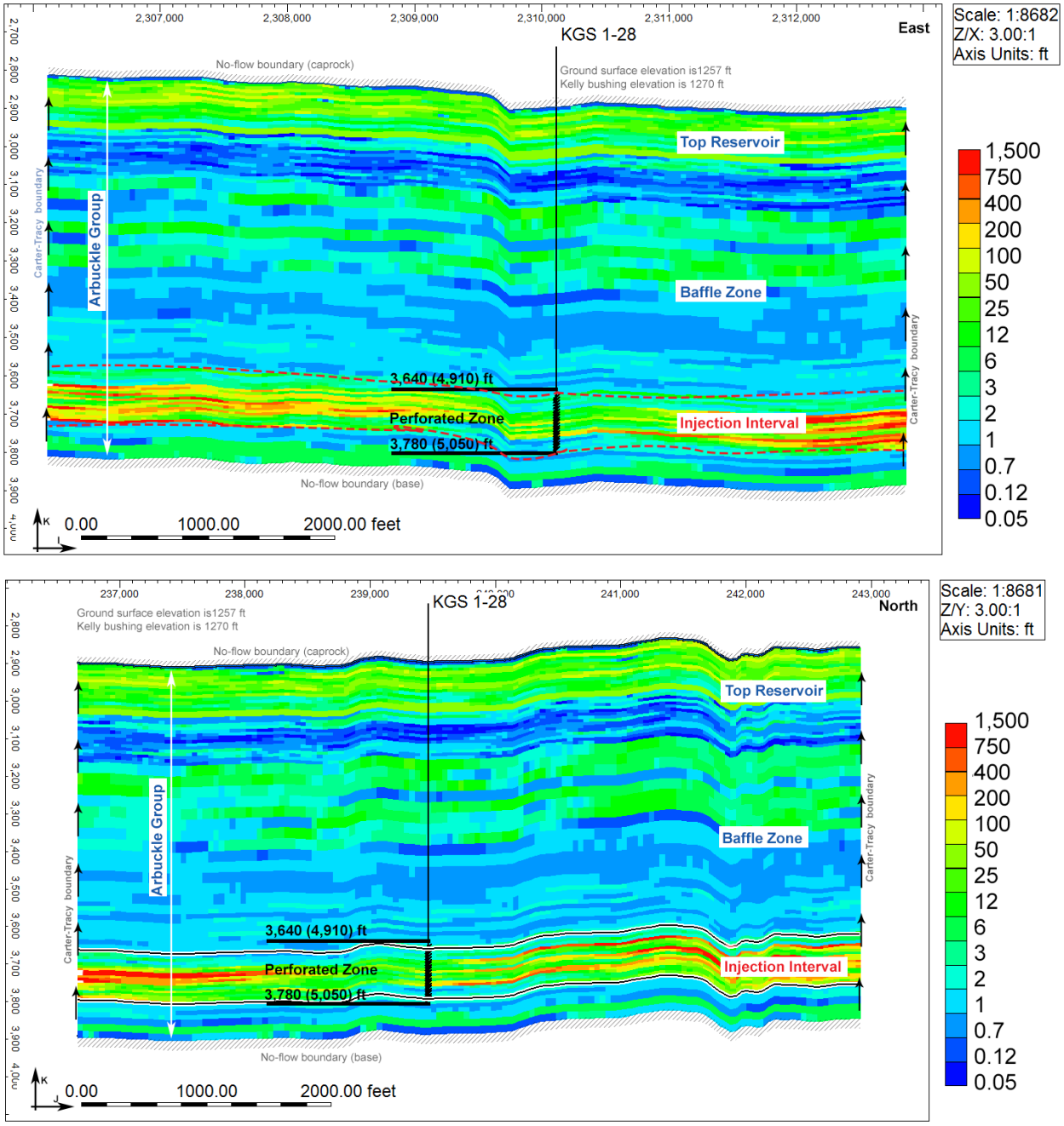

Figure 7. Upscaled horizontal permeability distribution (mD) in an E-W (top) and N-S (orientation) through the injection well. The locations of the cross sections are shown in Figure 2.

Vertical Permeability Images:

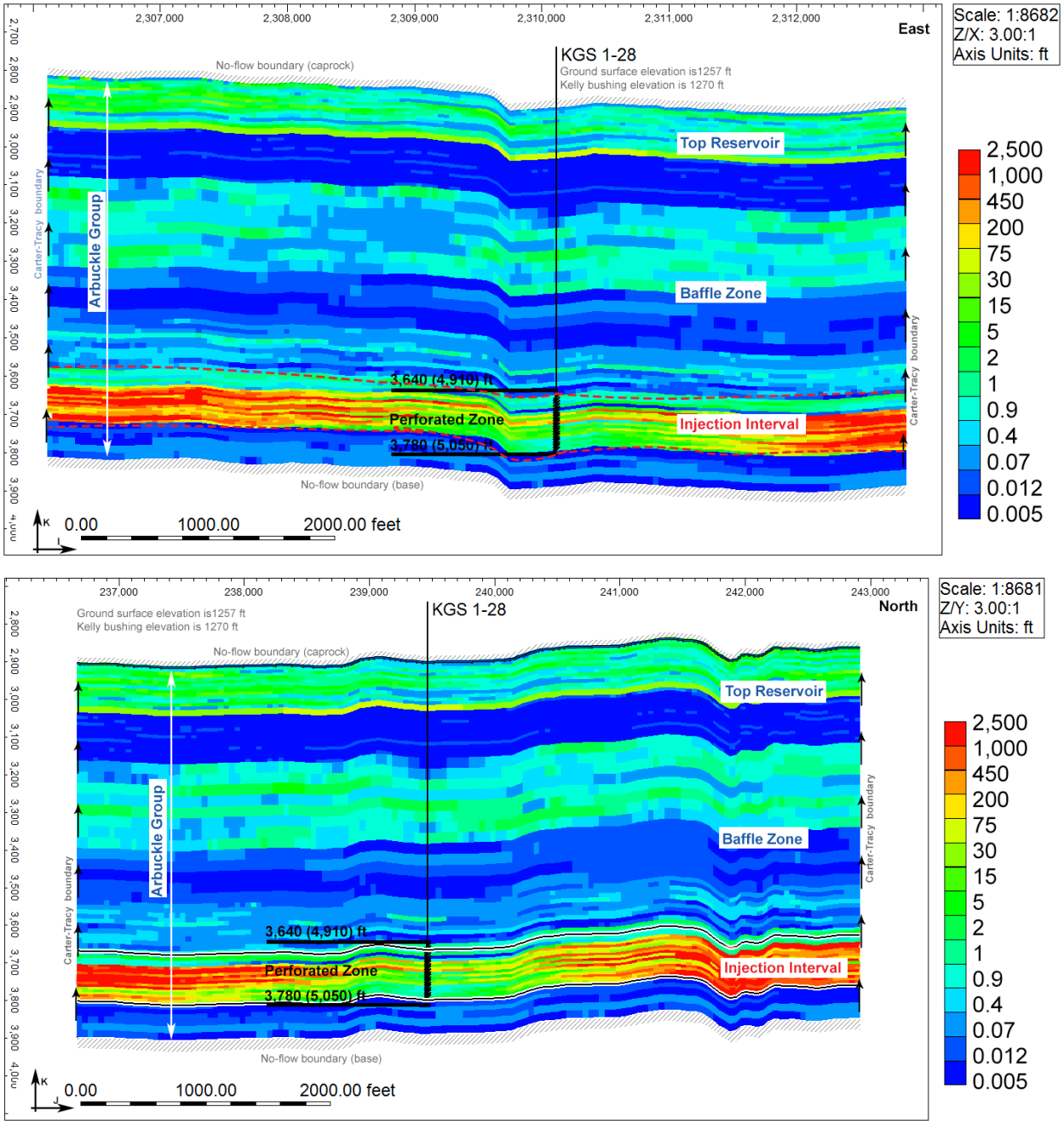

Figure 8. Upscaled vertical permeability distribution (mD) in an E-W (top) and N-S (orientation) through the injection well. The locations of the cross sections are shown in Figure 2.

The permeability in most of the Arbuckle Group KGS 1-28 and 1-32 is within the 1-10 mD range. This is based on NMR-based porosity estimates that generally agree well with core-based laboratory results. The core-based estimates are biased to the low end of the permeability range due to the tendency of samples to be collected in tight rock. The log-based horizontal permeability distribution is in agreement with permeability estimates for the Arbuckle obtained

from various sources. Flow Zone Indicator (FZI) was used to estimate the permeability for intervals of the injection zone in KGS 1-32 where whole core measurements were not possible due to broken core or to lack of recovery.

The distribution of the nine rock types in the geological model is presented in Figure 9.

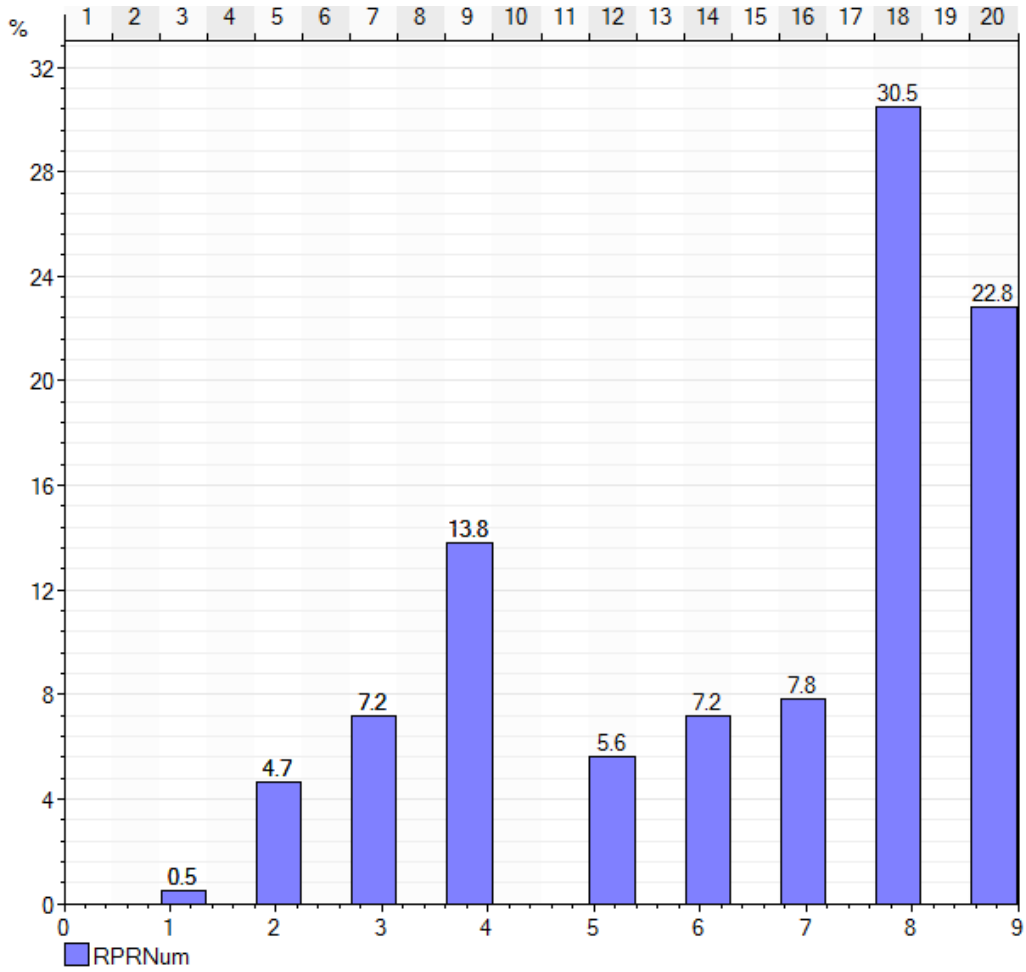

Figure 9. Schlumberger's Petrel-generated histogram for the rock type distribution based on the geological model used to calculate porosity and permeability.

Constitutive Relationships

Rock types were determined based on reservoir quality index (RQI) ranges and assigned using CMG Builder's Formula Manager and distributed throughout the model grid by the model. Nine rock types were included and nine sets of relative permeability curves for both drainage and imbibition were calculated (one for each type). These curves were calculated based on a recently patented formula (SMH reference No: 1002061-0002) that relates end-points to RQI. The highest and lowest Corey CO_2 exponent values from Bennion and Bachu (2010)[9] were selected and

[9] Bennion, D., and Bachu, S., 2010. Drainage and Imbibition CO2/Brine Relative Permeability Curves at Reservoir Conditions for Carbonate Formations. SPE Publication 134028.

assigned to the nine RQIs in a descending order from high to low (i.e., highest RQI to lowest). Corey water exponents for different permeabilities from the literature did not show much variability. Therefore, average values were used for both drainage and imbibition curves. Residual CO_2 saturation was needed to calculate imbibition curves, and was calculated based on a correlation between residual CO_2 saturation and initial CO_2 saturation.[10] Relative permeability curves for the full range of RQIs are presented in Figure 10 and Appendix 1. Capillary pressure curves for each of the nine rock types was also calculated using the method referenced above (SMH reference No: 1002061-0002). The formula constitutes a function for the shape of capillary pressure curves and functions for the end-points of entry pressure and irreducible water saturation. The end-points are correlated to RQI. The entry pressure was calculated from entry radius (R15) and Winland R35. Irreducible water saturation was calculated from the NMR log at a capillary pressure equal to 20 bars.

The capillary pressure and relative permeability curves were estimated in the laboratory for the Mississippian Reservoir as part of the Wellington Mississippian Enhanced Oil Recovery project located approximately a mile southwest of the Wellington CO_2 storage site. The laboratory derived curves were used to validate the relative permeability and capillary pressure approach used for the Arbuckle (and described above). Two core plug samples with similar RQI were sent for laboratory capillary pressure and relative permeability measurements. The relative permeability and capillary pressure curves were calculated twice for the Mississippian – prior to and following the core results from the laboratory. There was a slight difference between the calculated and measured capillary pressure before calibration, and an excellent match between calculated and measured capillary pressures after calibration using the core-measured endpoints.

[10] Burnside, NM & Naylor, M 2014, 'Review and implications of relative permeability of CO2/brine systems and residual trapping of CO2' International Journal of Greenhouse Gas Control, Volume 23, pp. 1-11.

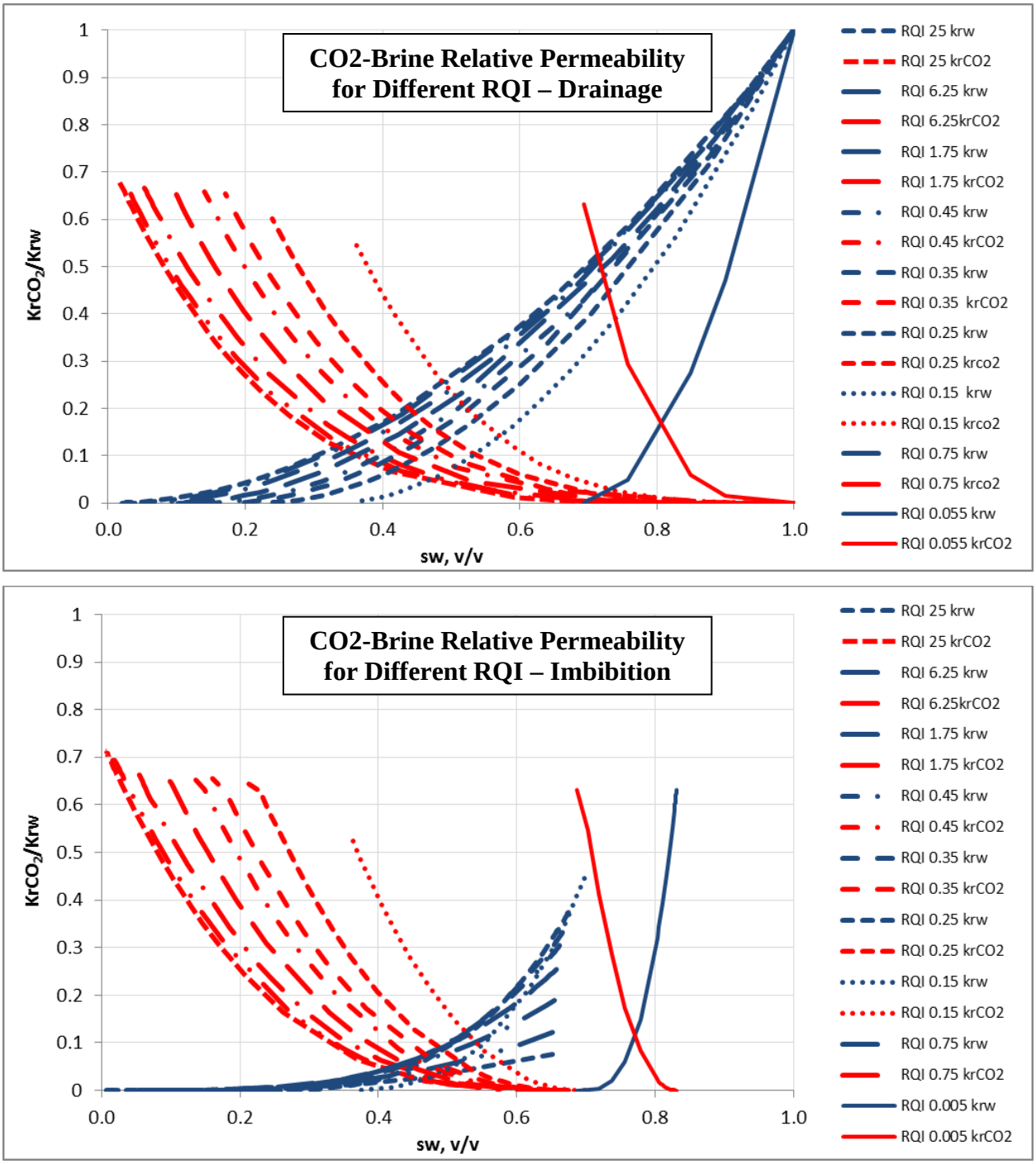

Figure 10. Calculated CO_2-brine relative permeability for drainage (top) and imbibition (bottom) for the full set of RQI.

Boundary Conditions

No-flow boundaries were specified at the top and bottom of the Arbuckle (immediately below the confining zone and immediately above the Precambrian basement). Preliminary simulations indicated that the bulk of CO_2 will remain confined in the lower portions of the Arbuckle

because of the low permeability intervals in the baffle zones which was demonstrated in analysis of geologic logs at wells KGS 1-28 and 1-32. The specification of a no-flow boundary at the top of the Arbuckle is also in agreement with hydrogeologic analyses, which indicate that the upper confining zone – comprising the Simpson Group, the Chattanooga Shale, and the Pierson formation – has very low permeability, which should impede any vertical movement of groundwater from the Arbuckle. A no-flow boundary is appropriate at the bottom of the injection formation because the presence of the Precambrian granitic basement under the Arbuckle is expected to provide hydraulic confinement.

The lateral boundary conditions were set as an infinite-acting Carter-Tracy aquifer with leakage.[11,12] This is appropriate since the Arbuckle is an open hydrologic system extending over most of Kansas. The suitability of applying a Carter-Tracy boundary for hydrogeologic simulations has also been demonstrated by Kipp (1986).[13]

Initial Conditions

Initial conditions for the model are given in Table 4.

Table 4. Initial conditions.

Parameter	Value
Initial aqueous pressure (varying with depth, temperature, and salinity)	2,093 psi (at -4,960 ft KB)
Initial temperature (spatially constant)	140° F
Initial salinity (spatially constant)	140 g/L
Fluid density	68.64 lbs/ft^3

Berexco plans a "cold injection" scheme in which liquid CO_2 is injected without prior heating, and the injection temperature is expected to be -10°F; however, modeled injection temperature is 140°F for the AoR delineation. The simulations were conducted assuming isothermal conditions with a constant spatial temperature of 140°F. Constant spatial temperature was used due to the narrow injection zone, where the gradient of temperature is not significant enough to impact the calculation of petrophysical properties. This was determined through log analysis and other temperature gradient calculations. Since it is forecasted that the CO_2 will not escape the injection zone, it is reasonable to apply the spatially constant temperature of 140°F. Furthermore, Berexco conducted non-isothermal sensitivity analyses using CMG's GEM software to demonstrate that varying temperature only minimally impacts the plume extent and pressure distribution. There are three predominant rock types which were populated for the injection zone (types 2, 3, and 4

[11] Dake, L. P., 1978, Fundamentals of Reservoir Engineering," Chapter 9, Elsevier Scientific Publishing Co., 1978.

[12] Carter, R. D., and Tracy, G. W., 1960. An improved method for calculating water influx, Petroleum Transactions, AIME, Volume 219, p. 415-417

[13] Kipp, K. L., 1986. Adaptation of the Carter-Tracy Water Influx Calculation to Groundwater Flow Simulation, Water Resources Research, Volume 22, Issue 3, pages 423-428.

on the RQI scale) and to decrease computational time, Berexco used only Rock Type 2 throughout the reservoir for the non-isothermal simulation.

Operational Information

Details on the injection operation and Arbuckle monitoring well are presented in Table 5.

Table 5. Operating details.

Operating Information	**KGS 1-28**
Location (global coordinates) X Y	 37.319485 97.4334588
Model coordinates (ft) X Y	 2,310,119 239,467
No. of perforated intervals	1 (140 ft)
Perforated interval (ft KB) Z top Z bottom	 4,910 5,050
Wellbore diameter (in.)	5.5
Planned injection period Start End	 09/2016 06/2017
Injection duration	9 months
Injection rate for 26K scenario	96.3 MT[1]/day
Injection rate for 40K scenario	150 MT[1]/day
Maximum injection volume	26,000 MT or 40,000 MT
Monitoring Information	**KGS 2-28**
Location (global coordinates) X Y	-97.435116, 37.320023

[1]MT: Metric tons

Fracture Pressure and Fracture Gradient

Calculated fracture gradient and maximum injection pressure values are given in Table 6. The maximum allowable bottomhole injection pressure of 2,651 psi in the permit reflects 70% of the estimated fracture gradient of 0.75 psi/ft (measured from the land surface) to minimize the risk of inducing a seismic event.

Table 6. Injection pressure details.

Injection Pressure Details	Injection Well 1
Fracture gradient (psi/ft)	0.75
Maximum bottomhole pressure (70% of fracture pressure) (psi)	2,651
Elevation corresponding to maximum injection pressure (ft KB)	5,050
Elevation at the top of the perforated interval (ft MSL)	4,910

The fracture gradient in Kansas is typically assumed to be 0.75 psi/ft by the Kansas Department of Health and Environment for the purposes of permitting Class I injection wells[14]. An estimate of the fracture gradient at the Wellington site was also obtained using the density log and pore pressure information at the injection well site (KGS 1-28). In a tectonically relaxed region such as Kansas, the fracture gradient can be estimated by Eaton's equation[15], which is a function of the overburden pressure, pore pressure, and Poisson's ratio:

$$F = \left(\frac{\vartheta}{1-v}\right)\left(\frac{P_{ob} - P_p}{D}\right) + \left(\frac{P_p}{D}\right)$$

Where:

- F = fracture gradient (psi)
- ϑ = Poisson ratio
- P_{ob} = overburden pressure (psi)
- P_p = pore pressure of formation fluid (psi)
- D = depth (ft)

At the injection site, a pore pressure of 2090.25 psi was measured at a depth of 5,010 feet. Triaxial tests were conducted in KGS 1-32 (geologic test well) for 15 depths between 3,630 and 5,151. This depth range covers the confining zone and injection formation. An average Poisson ratio of 0.30 in the Arbuckle was derived from laboratory analysis of these core samples. Based on Eaton's equation shown above, a fracture gradient of 0.72 psi/ft is derived, fairly close to the 0.75 psi/ft assumed for this project.

Injection pressure will be monitored during operation (see Attachment C, the Testing and Monitoring Plan) to ensure that the fracture pressure of the formation and the burst pressure of the well tubing are not exceeded. Situations that will trigger an AoR reevaluation are described later in this plan. These include an increase in pressure that exceeds 70% of the fracture gradient.

[14] Kansas Department of Health and Environment (KDHE), 2013, Email communication with Michael Cochran, Chief, Geology Section, dated February 9, 2013.

[15] Eaton, B. A., 1969, Fracture gradient prediction and its application in oilfield operations: Journal of Petroleum Technology, v. 21, p. 1,353–1,360.

Computational Modeling Results

Predictions of System Behavior

NOTE: Although Berexco is permitted to inject 40,000 MT, it is likely that only 26,000 MT will be injected. Based on Berexco's anticipated injection volume, at the request of EPA, an alternate set of simulations was modeled with a total injection mass of 26,000 MT to provide a baseline for AoR reevaluations, to provide predictions for comparison with testing and monitoring results, and to help support a non-endangerment demonstration at the end of the alternative post-injection site care (PISC) timeframe. The results of both simulations are presented here; the AoR is based on the 40,000 MT scenario, which produces the maximum extent of the separate-phase CO_2 plume.

A total of nine models representing three sets of alternate permeability-porosity combinations were simulated with the objective of bracketing the range of expected pressures and extent of CO_2 plume migration (Table 7). These nine models were run for both the 40,000 and 26,000 MT scenarios.

Table 7. Alternative porosity and permeability scenarios.

	75% of Base Porosity	Base Porosity	125% of Base Porosity
75% of Base Permeability	K-0.75/phi-0.75	K-0.75/phi-1.0	K-0.75/phi-1.25
Base Permeability	K-1.0/phi-0.75	K-1.0/phi-1.0	K-1.0/phi-1.25
125% of Base Permeability	K-1.25/phi-0.75	K-1.25/phi-1.0	K-1.25/phi-1.25

The high permeability/low porosity combination (k-1.25/phi-0.75) resulted in the largest lateral plume dimension. The highest induced pressures were obtained for the alternative model with the lowest permeability and lowest porosity (k-0.75/phi-0.75). Additional scenarios were defined for the purpose of sensitivity analyses, but AoR delineation was based on the scenarios listed in Table 7. Details on how this information was used to delineate the AoR is included in a later section of this Plan.

40,000 MT Injection Scenario – Maximum AoR Extent

The k-1.25/phi-0.75 alternative scenario results in the largest lateral plume migration. Results presented here represent this maximum scenario. At the end of the model timeframe (100 years) the separate-phase CO_2 plume extends approximately 4,300 ft in the NW-SE direction, and approximately 2,520 ft in the SW-NE direction (Figure 11). Both of these vectors represent the furthest extent of the plume. The plume is expected to reach its maximum extent in most directions by the end of the four-year PISC timeframe and thereafter will continue to exhibit slow growth in the northwest direction.

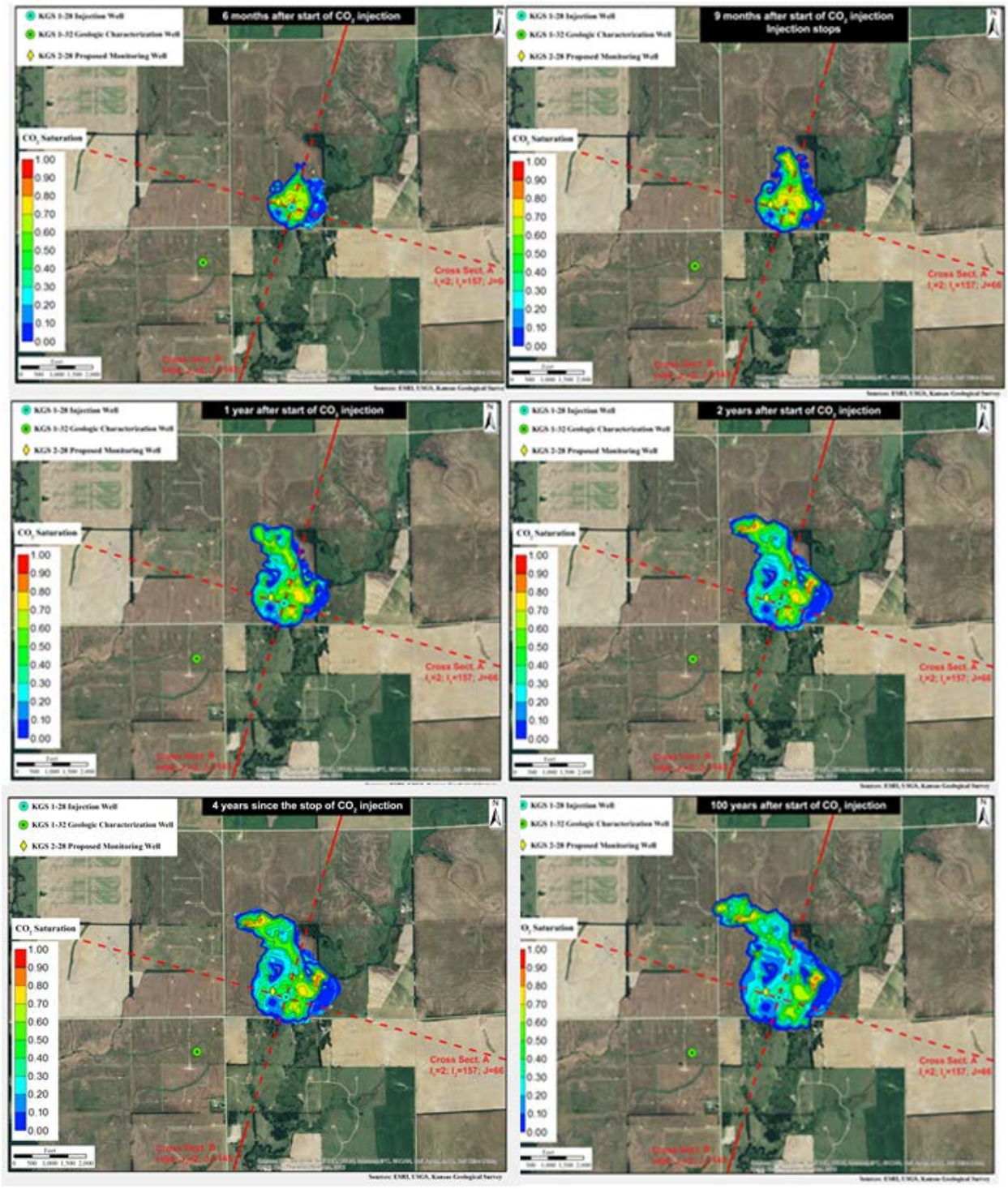

Figure 11. Evolution of the separate-phase plume for the 40,000 MT scenario in aerial view.

The extent of vertical plume migration is shown in Figure 12 and Figure 13. The free-phase plume remains confined in the injection interval (lower Arbuckle) because of the presence of the low-permeability baffle zones discussed earlier in this Plan. To account for uncertainties of CO_2 movement in the vertical direction, an alternate vertical permeability model was developed in which the vertical permeability parameter was increased by 50% along with a porosity of 75% (k-1.50/phi-0.75). The extent of vertical migration for this case is approximately 30 feet higher than other scenarios, but still does not penetrate the low permeability baffle zone in the middle of the Arbuckle.

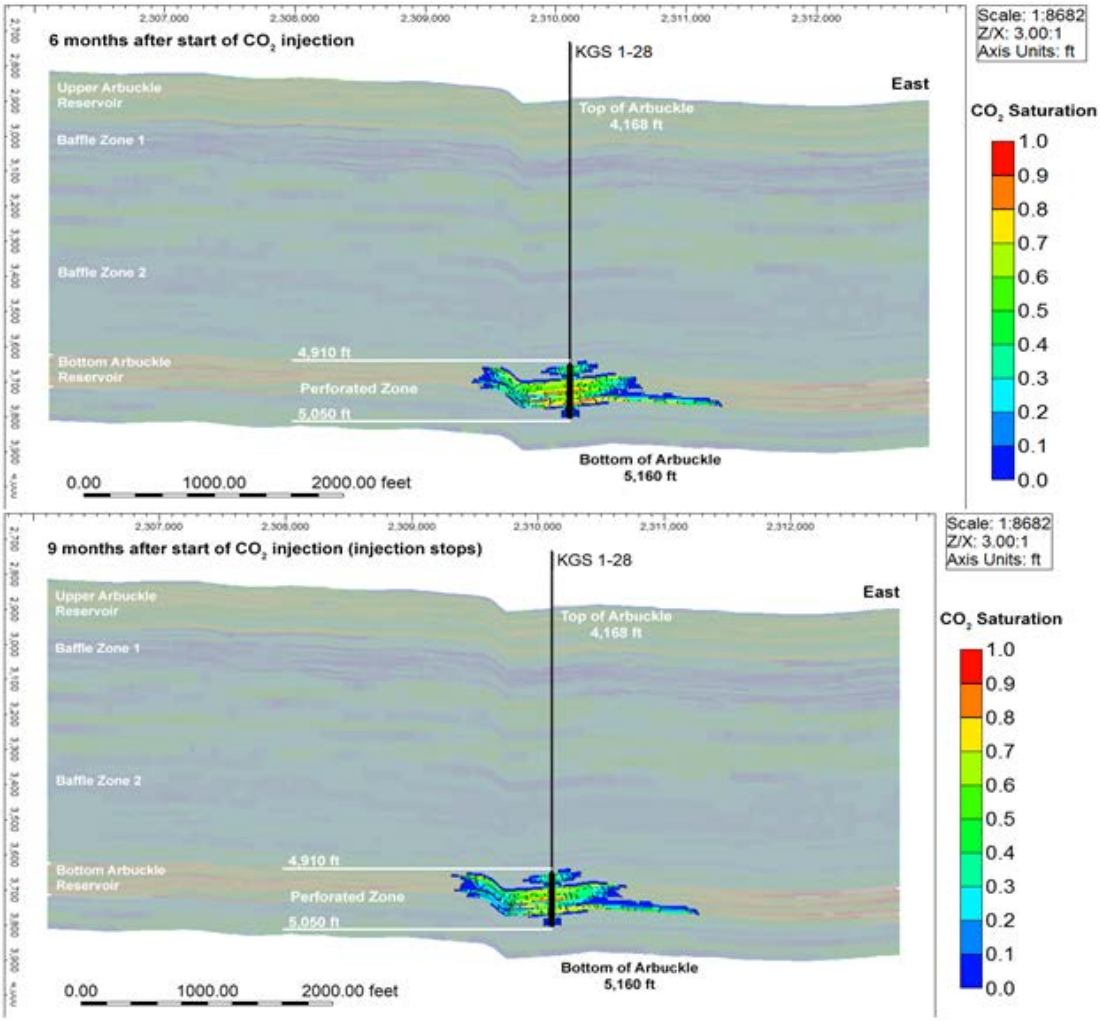

Figure 12a. E-W cross section showing vertical and lateral separate-phase plume migration at selected operational milestones for 40,000 tons injection (continued on the following page).

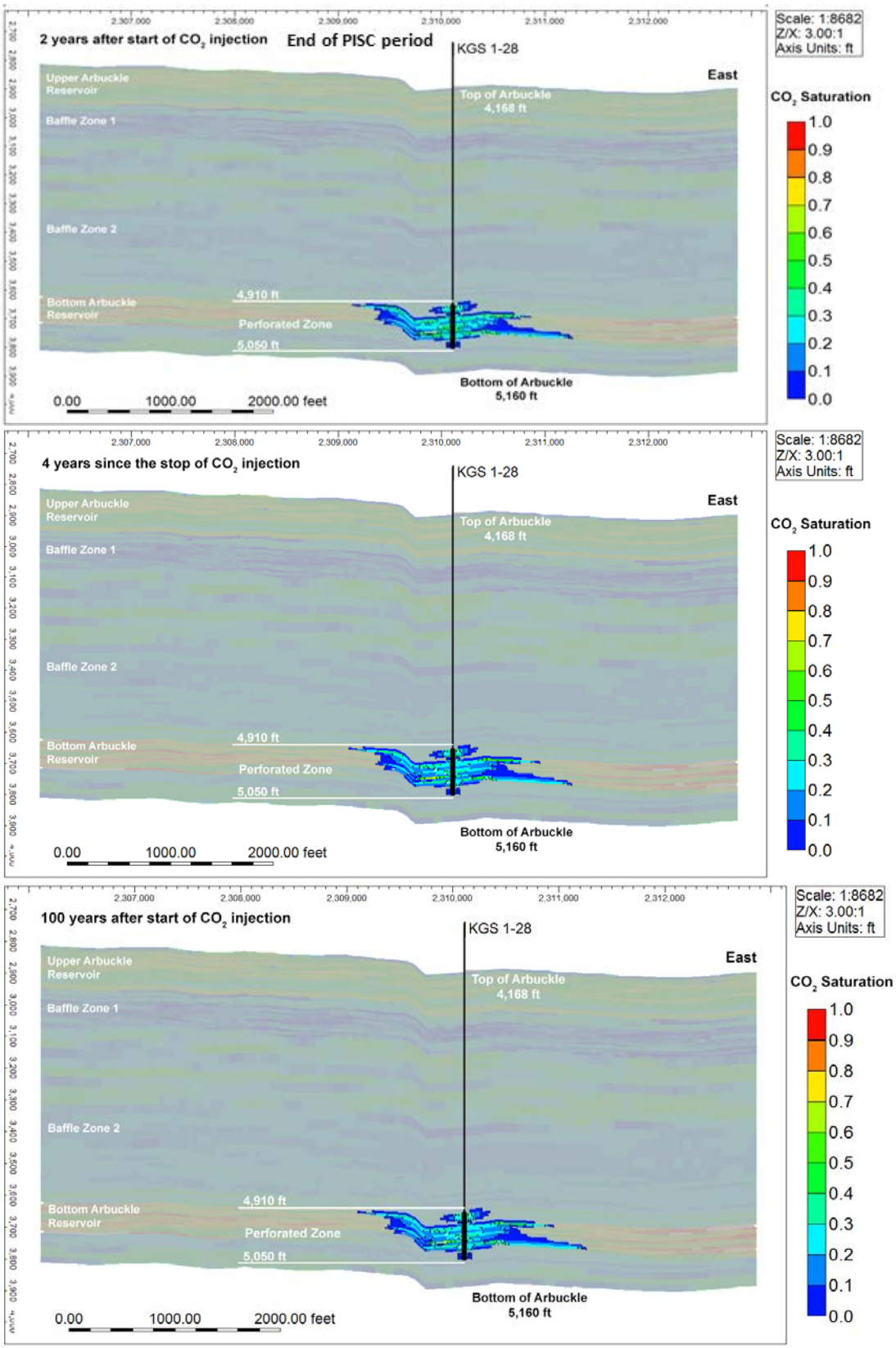

Figure 12b. E-W cross section showing vertical and lateral separate-phase plume migration at selected operational milestones for 40,000 tons injection (continued from the previous page).

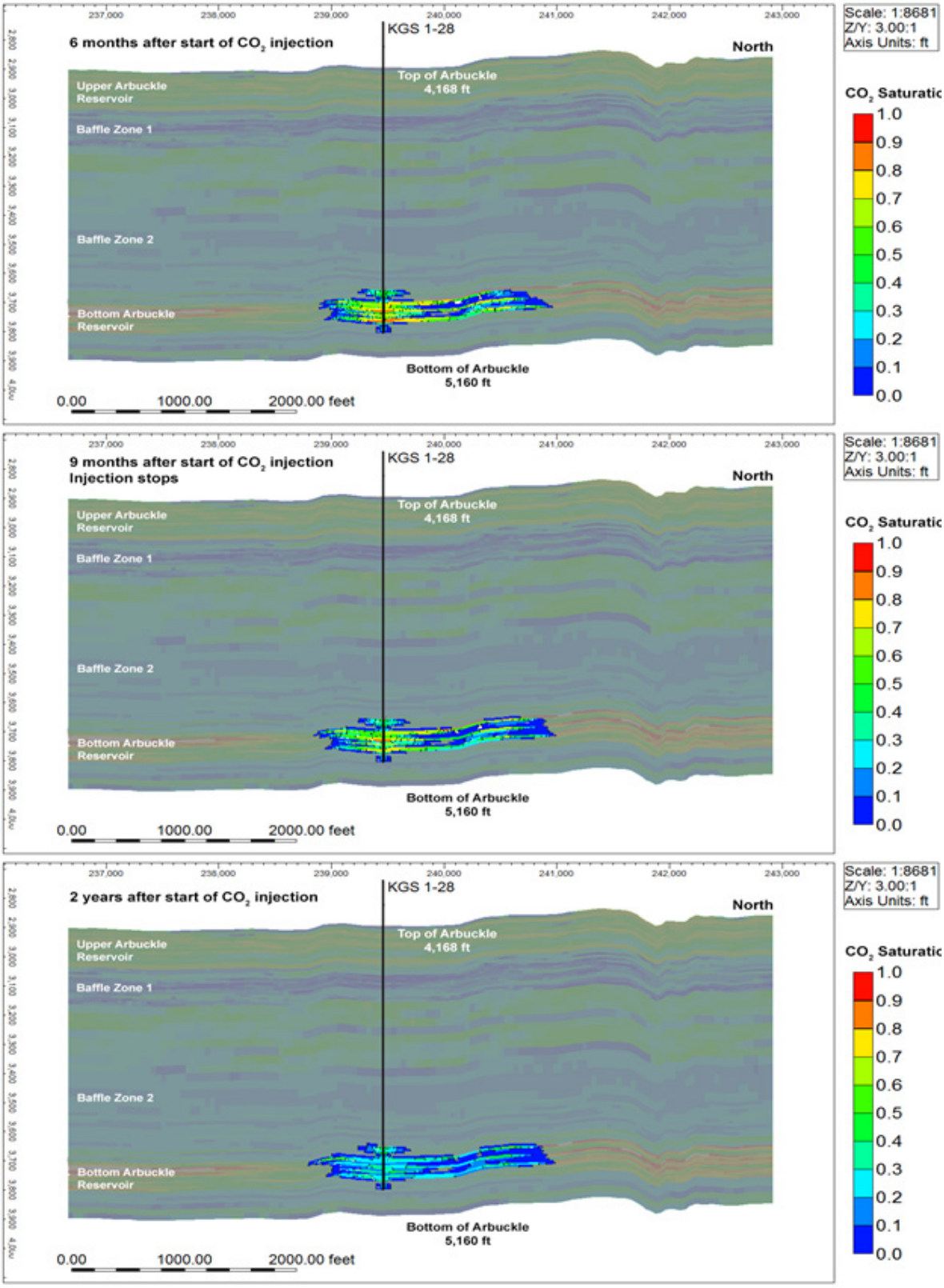

Figure 13a. N-S cross section showing vertical and lateral separate-phase plume migration at selected operational milestones for 40,000 tons injection (continued on the following page).

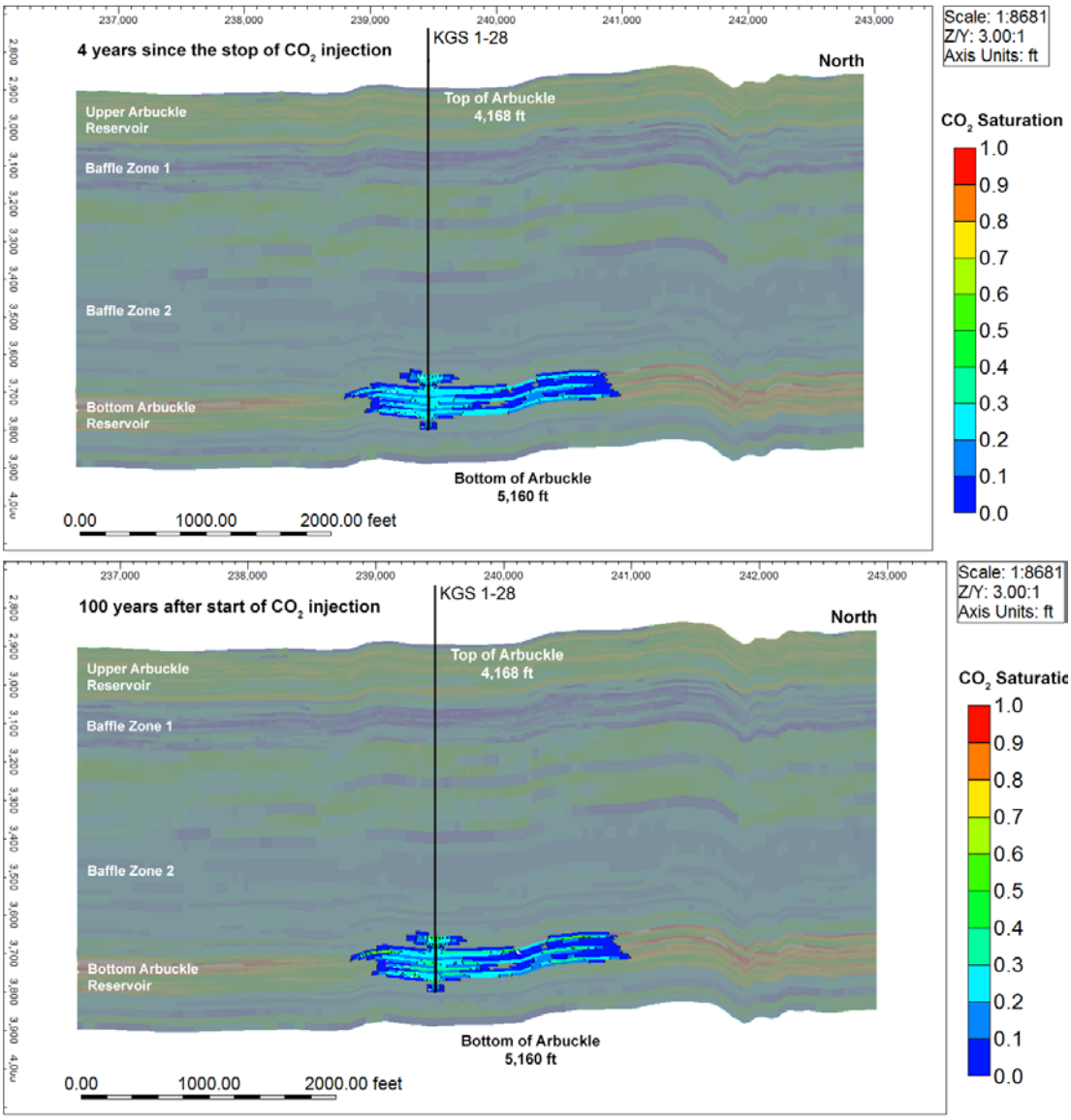

Figure 13b. N-S cross section showing vertical and lateral separate-phase plume migration at selected operational milestones for 40,000 tons injection (continued from the previous page).

The distribution of CO_2 phases (supercritical, trapped, and dissolved) for the total mass injection of 40,000 MT is presented in Figure 14. As discussed above, the AoR was defined based on the maximum extent of the separate-phase plume.

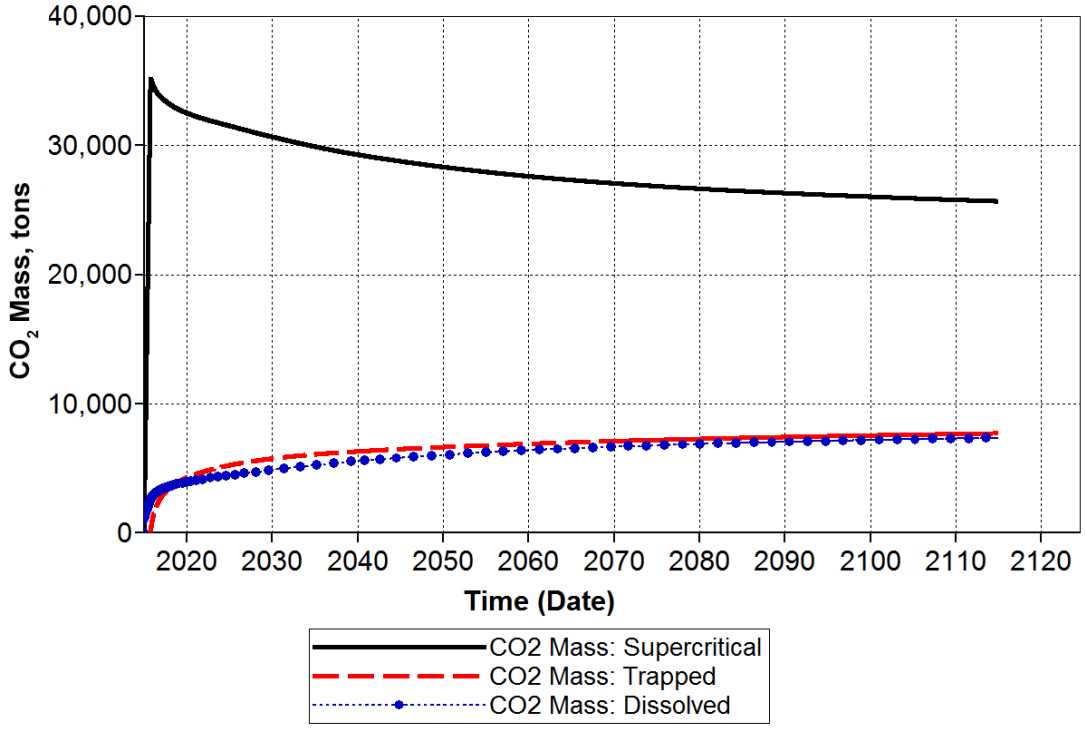

Figure 14. Mass partitioning in the model domain over time showing the change in integrated CO_2 mass in the gas, dissolved, and trapped phases for the 40,000 MT scenario.

The highest pressure alternative model was the k-0.75/phi-0.75 case. Under this scenario, the bottomhole pressure increases to 2,485 psi on commencement of injection and then gradually drops during the injection period as the capillary effects are overcome. The pressure drops significantly by the end of the first year after cessation of injection (Figure 15). The rise in pressure to 2,485 psi represents an increase of 392 psi over pre-injection levels and results in a pressure gradient of 0.515 psi/ft, which is less than the maximum allowable pressure gradient of 0.525 psi/ft (70% of fracture pressure).

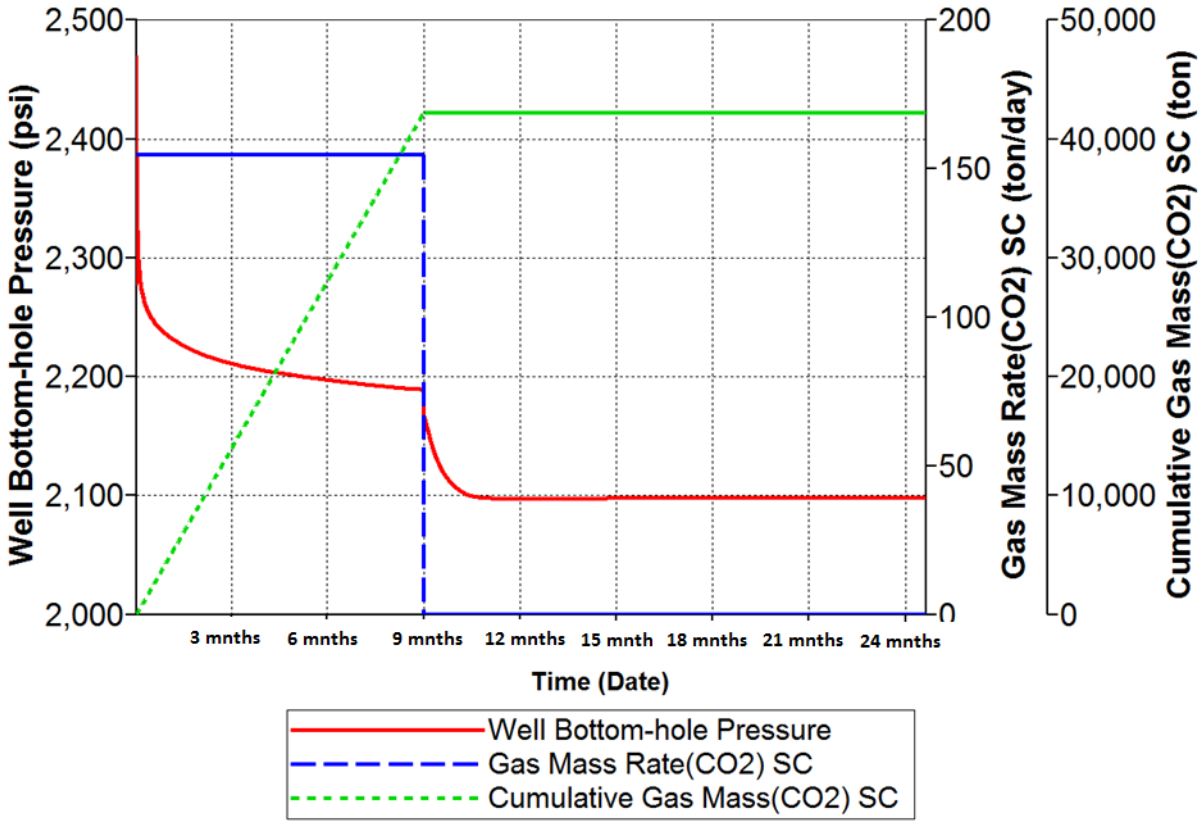

Figure 15. Maximum bottomhole pressure at a depth of 5,050 feet for the minimum porosity and minimum permeability scenario (k-0.75/phi-0.75) for the 40,000 MT scenario.

The lateral distribution of pressure and the rapid drop in pore pressure with distance from the injection well are illustrated in Figure 16. The lateral pressure front increases from commencement of injection to end of injection and then drops significantly by the end of the first year after cessation of injection. The pressures also drop very rapidly at short distances from the injection well.

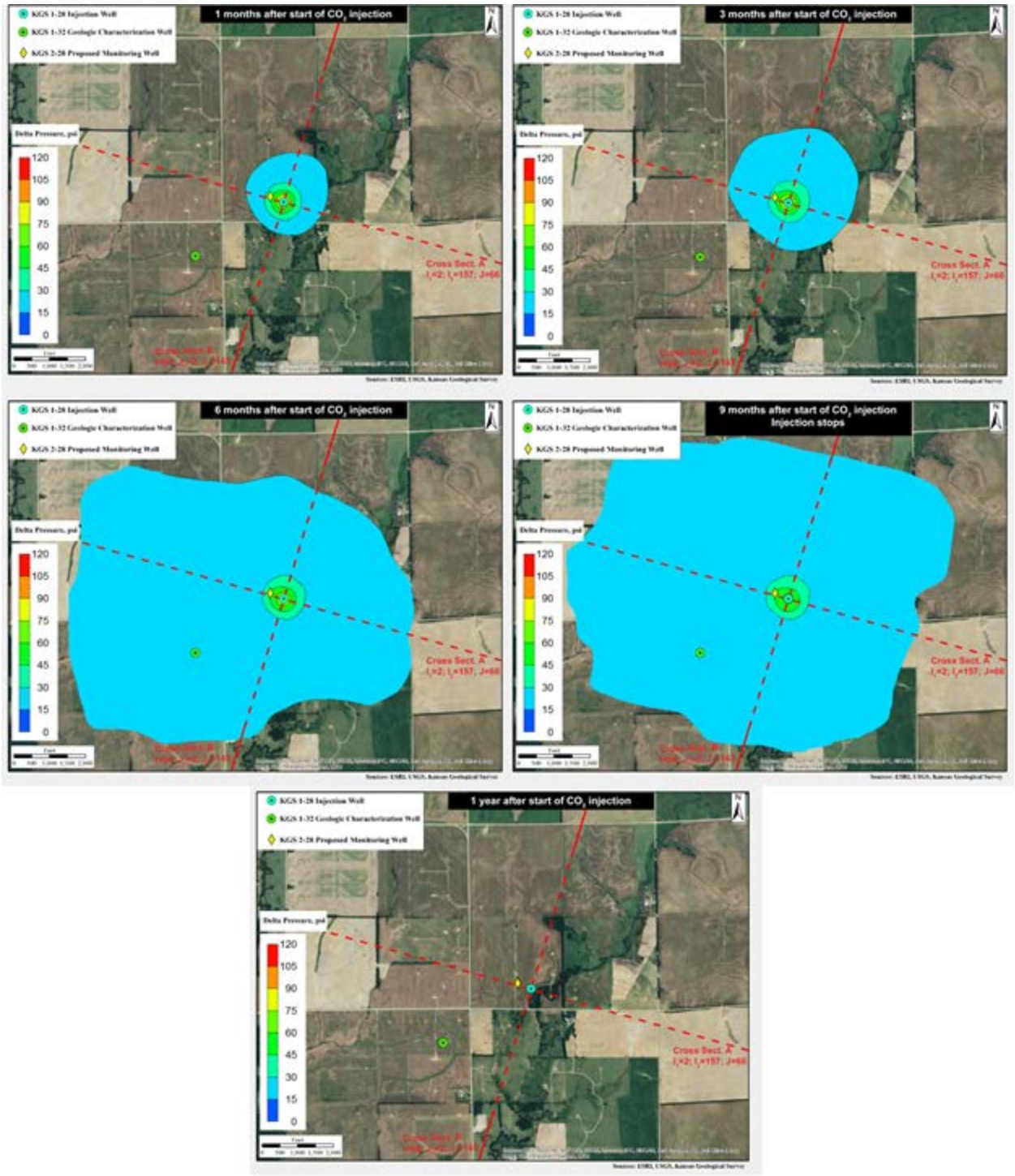

Figure 16. Evolution of the pressure front over time for the 40,000 MT scenario.

The confining effect of the mid-Arbuckle baffle zones is evident in the vertical pressure distribution at the end of the injection period as shown in Figure 17. The pressure declines rapidly at short distances from the injection well, and subsides to near pre-injection levels soon after the cessation of injection.

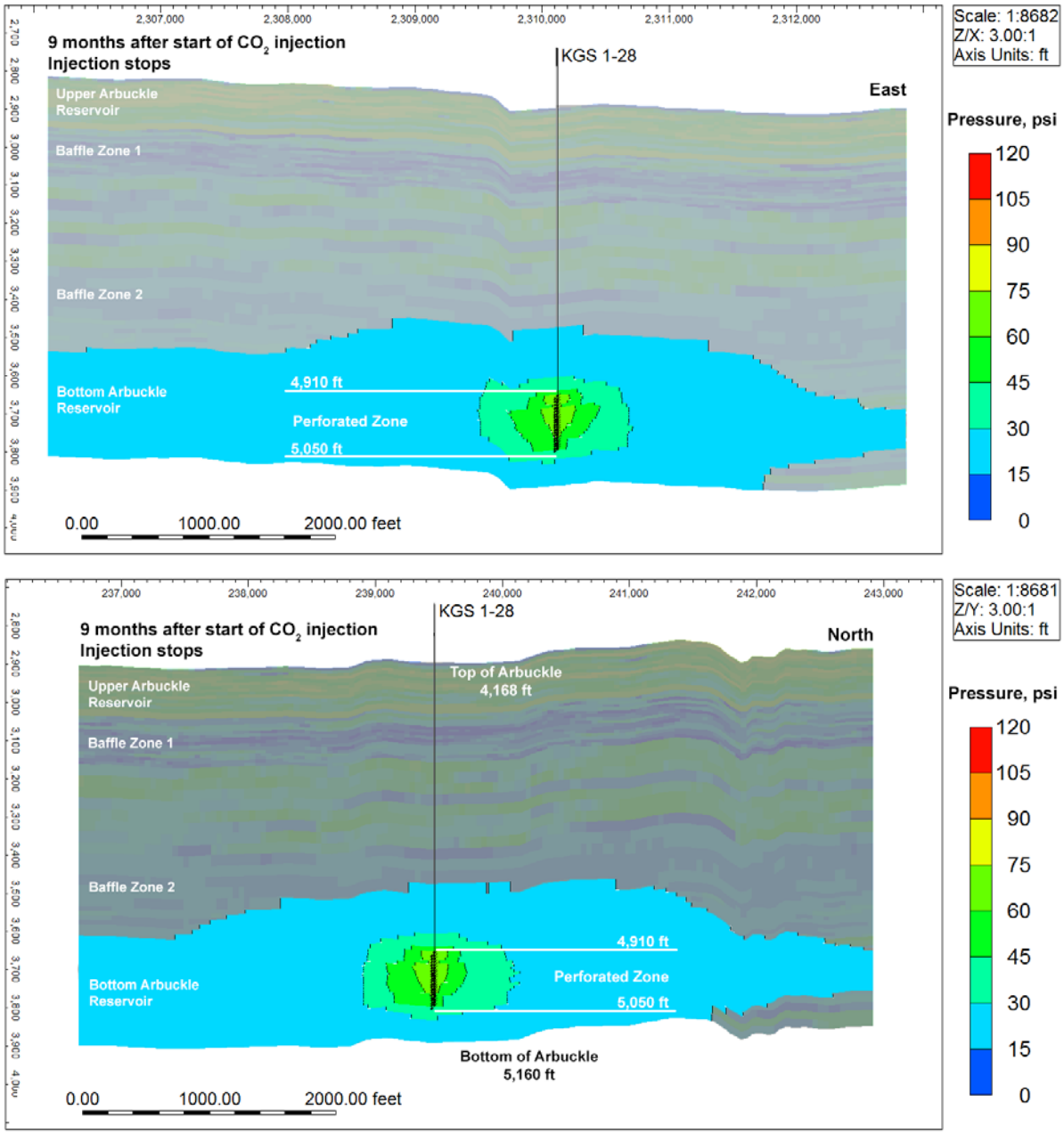

Figure 17. Maximum extent of the pressure front in the E-W (top) and N-S (bottom) orientations at the end of the injection period for the 40,000 MT scenario.

The simulation results discussed in this plan are expected to represent conservative estimates of plume migration. This is because the present simulations neglect mineral sequestration trapping and also use the "worst-case scenario"[16] to define maximum plume extent. Figure 18 and Figure

[16] This term, used in the permit application, refers to the conditions that result in the greatest plume migration or the highest induced pressure.

19 show the maximum plume extent at the end of the alternative PISC timeframe (which is 4 years after injection ends), and at the end of the 100-year model period, respectively.

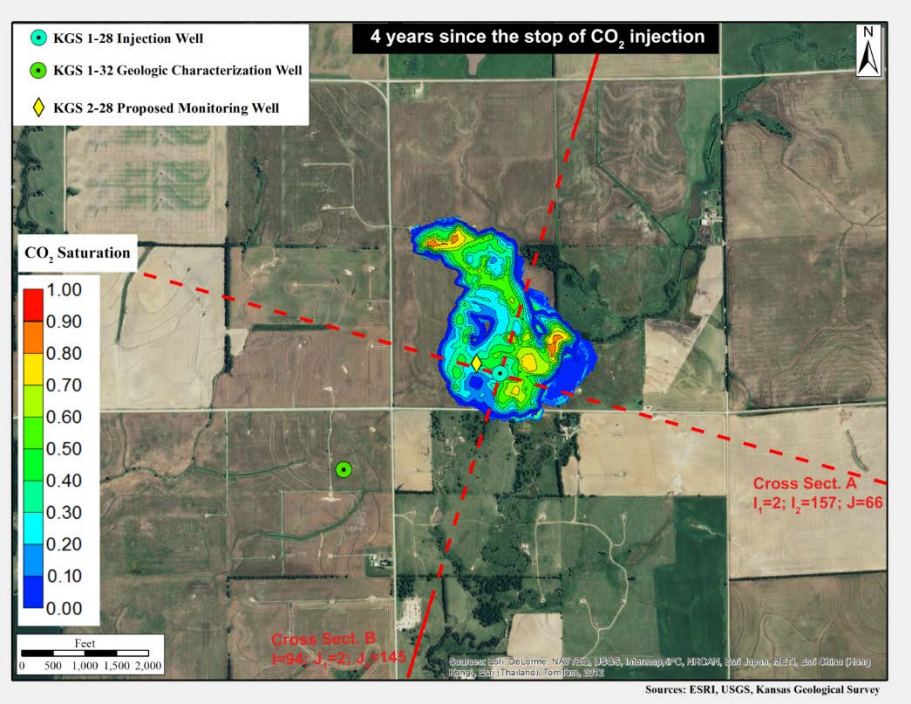

Figure 18. Separate-phase plume extent at the end of the alternative PISC timeframe (4 years after the cessation of injection) for the 40,000 MT scenario.

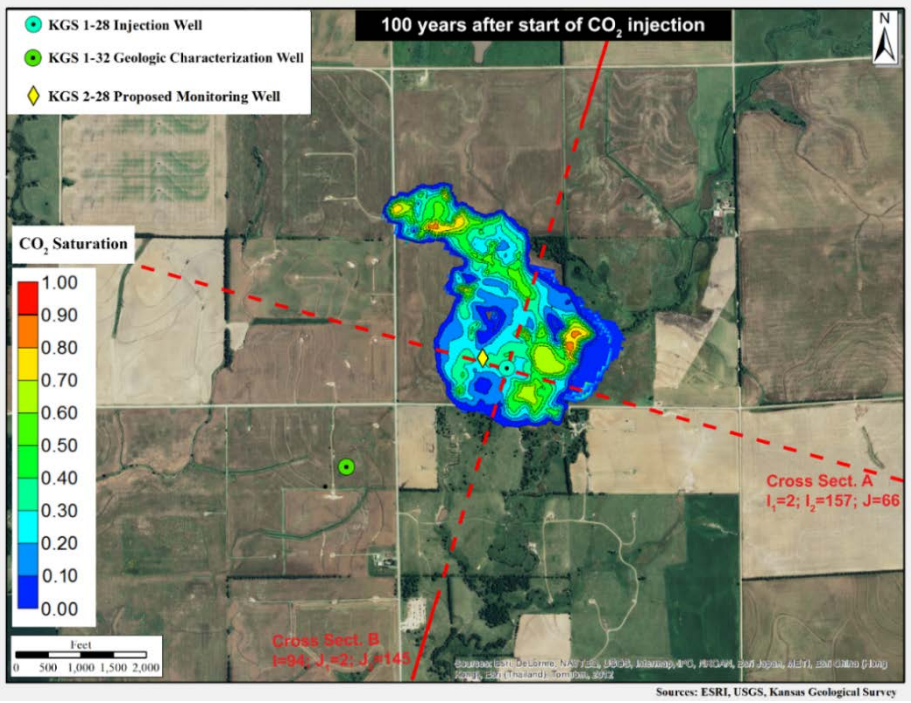

Figure 19. Maximum extent of plume migration at the end of the model period for the 40,000 MT scenario.

26,000 MT Injection Scenario – Expected Operational Conditions

The maximum plume extent for the 26,000 MT scenario (expected total injection volume) occurred under the largest areal migration case (k-1.25/phi-0.75). The plume at the end of 100 years has a maximum lateral spread of approximately 3,100 feet from the injection well (Figure 20). The plume is expected to reach its maximum extent in most directions by the end of the four-year PISC timeframe and thereafter will continue to exhibit slow growth in the northwest direction.

It is projected that the CO_2 front will arrive at the Arbuckle observation well (KGS 2-28) within the first or second month after the start of CO_2 injection.

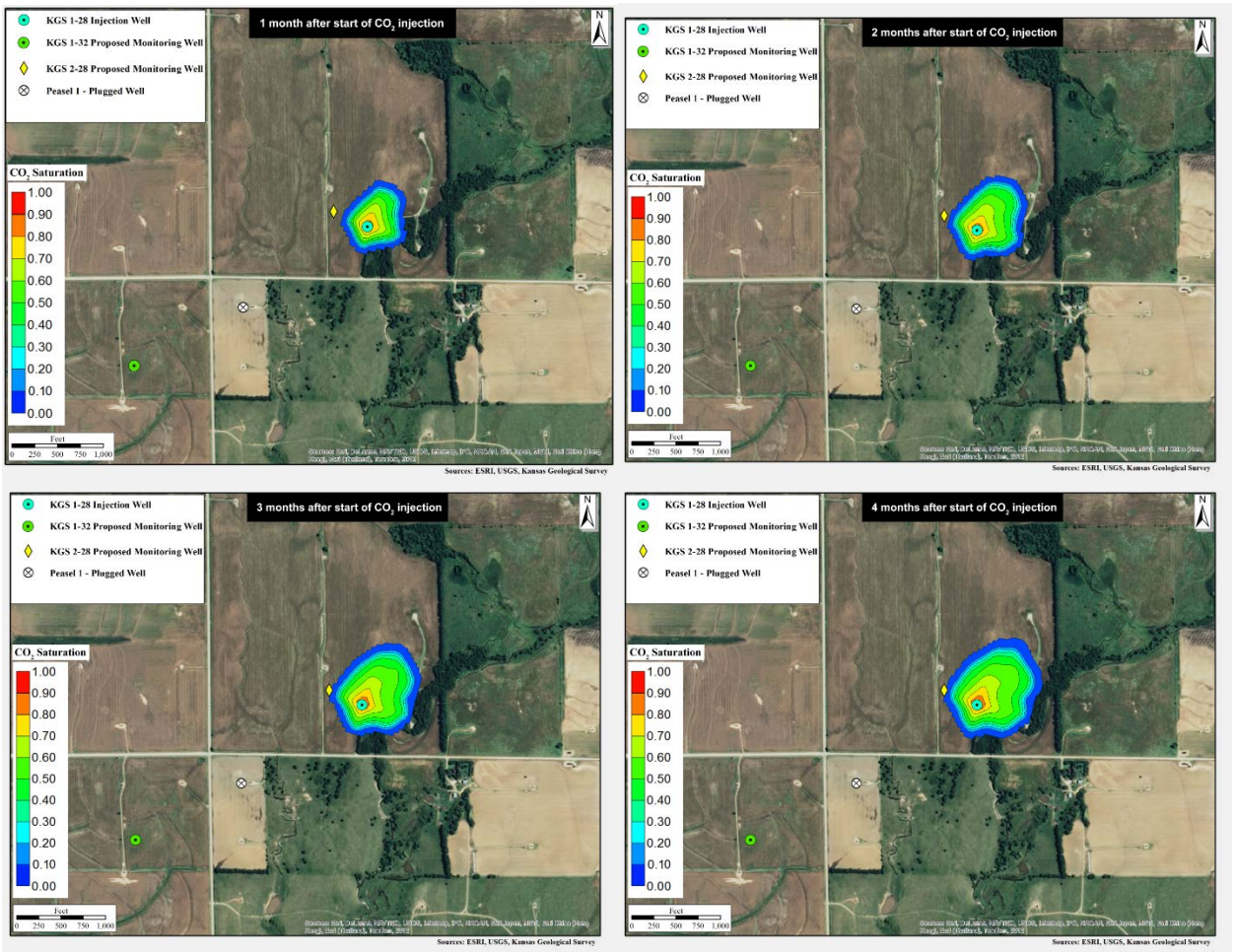

Figure 20a. Evolution of the separate-phase plume for the 26,000 MT scenario in aerial view (continued on the following page).

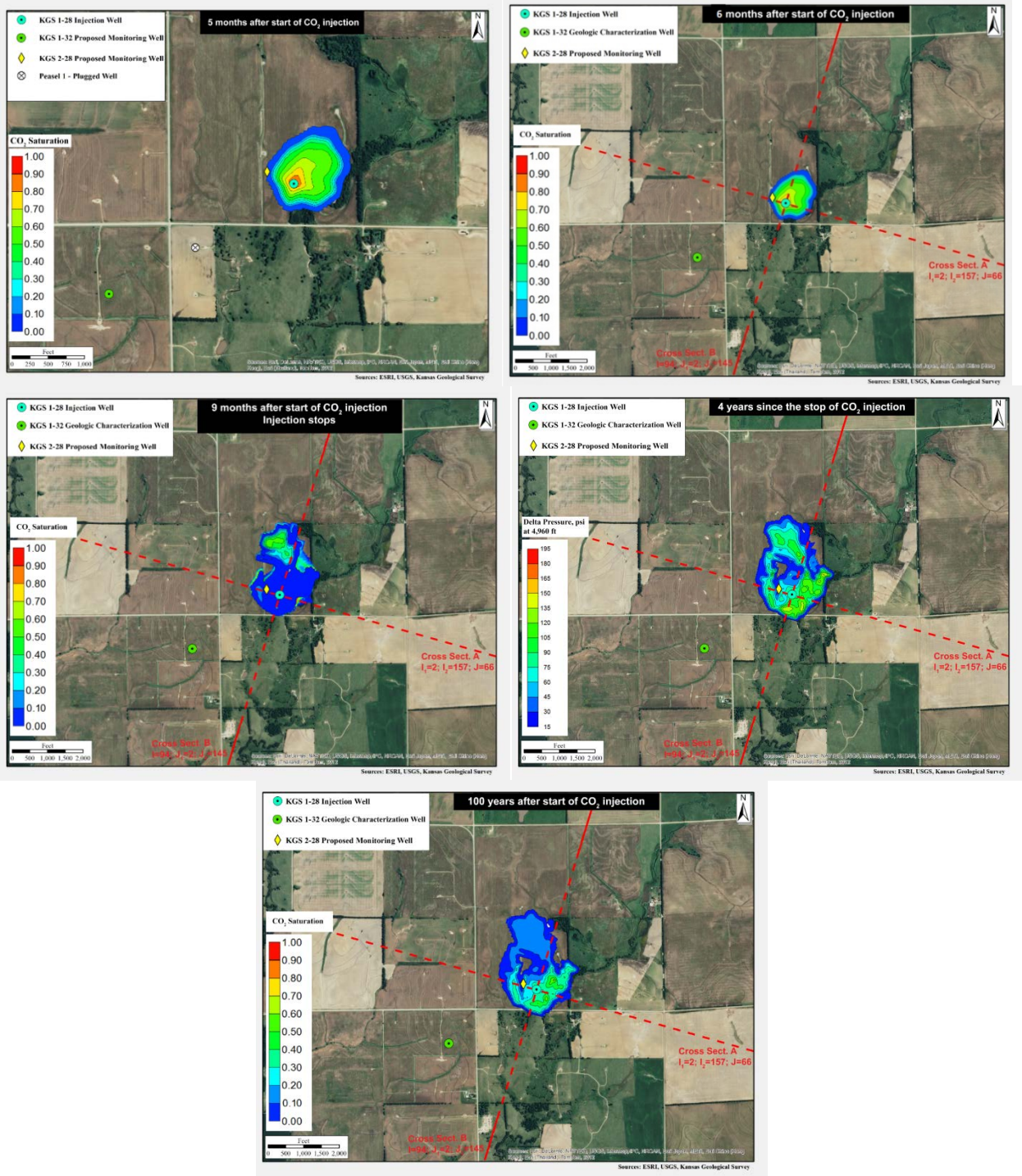

Figure 20b. Evolution of the separate-phase plume for the 26,000 MT scenario in aerial view (continued from the previous page).

In all modeled scenarios, the plume remains confined in the injection interval (lower Arbuckle) due to the presence of the low-permeability baffle zones described earlier in this plan. Figure 21 and Figure 22 show the vertical migration of the plume over time.

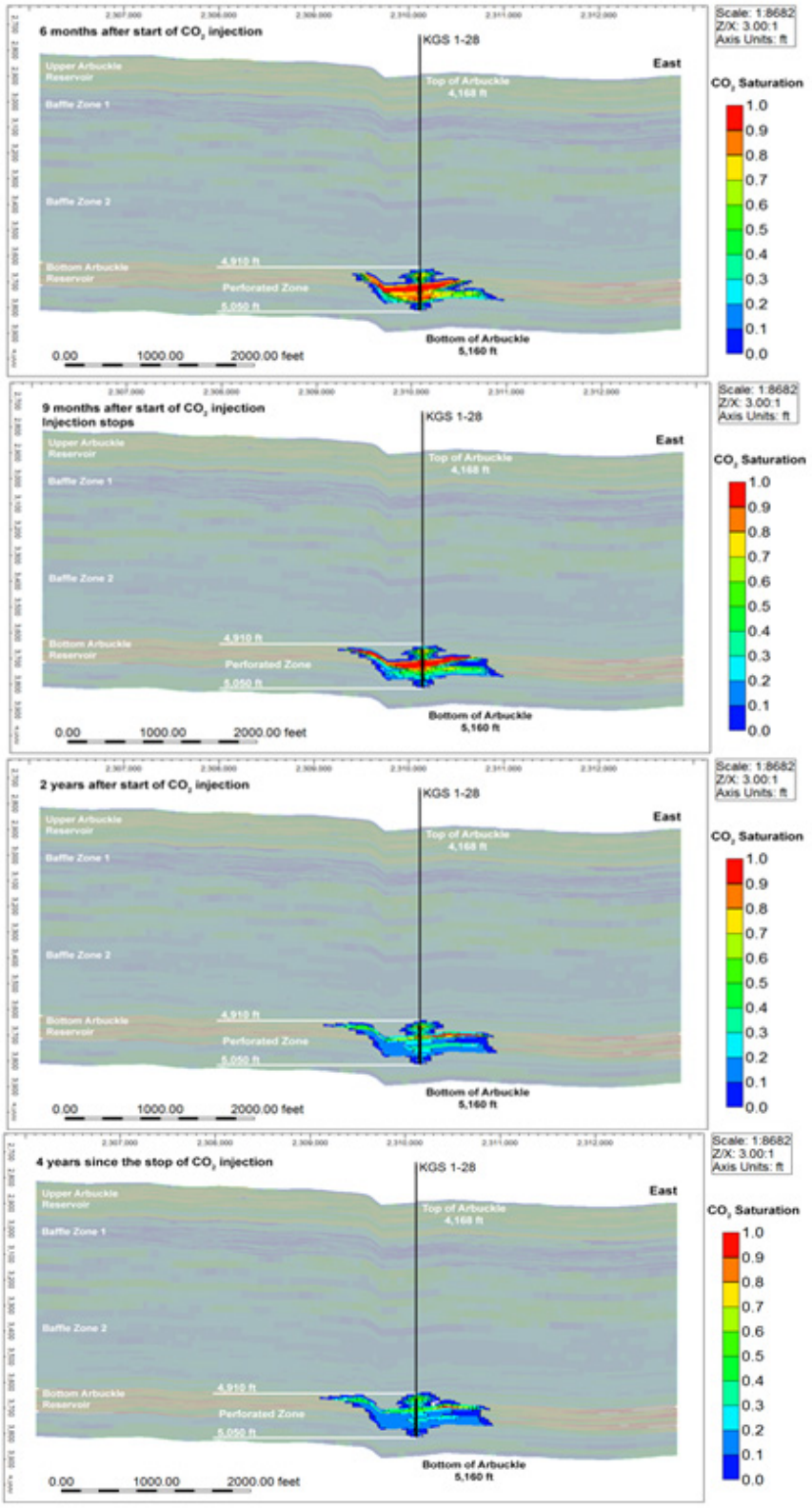

Figure 21. E-W cross section showing vertical and lateral separate-phase plume migration at selected operational milestones for the 26,000 MT scenario.

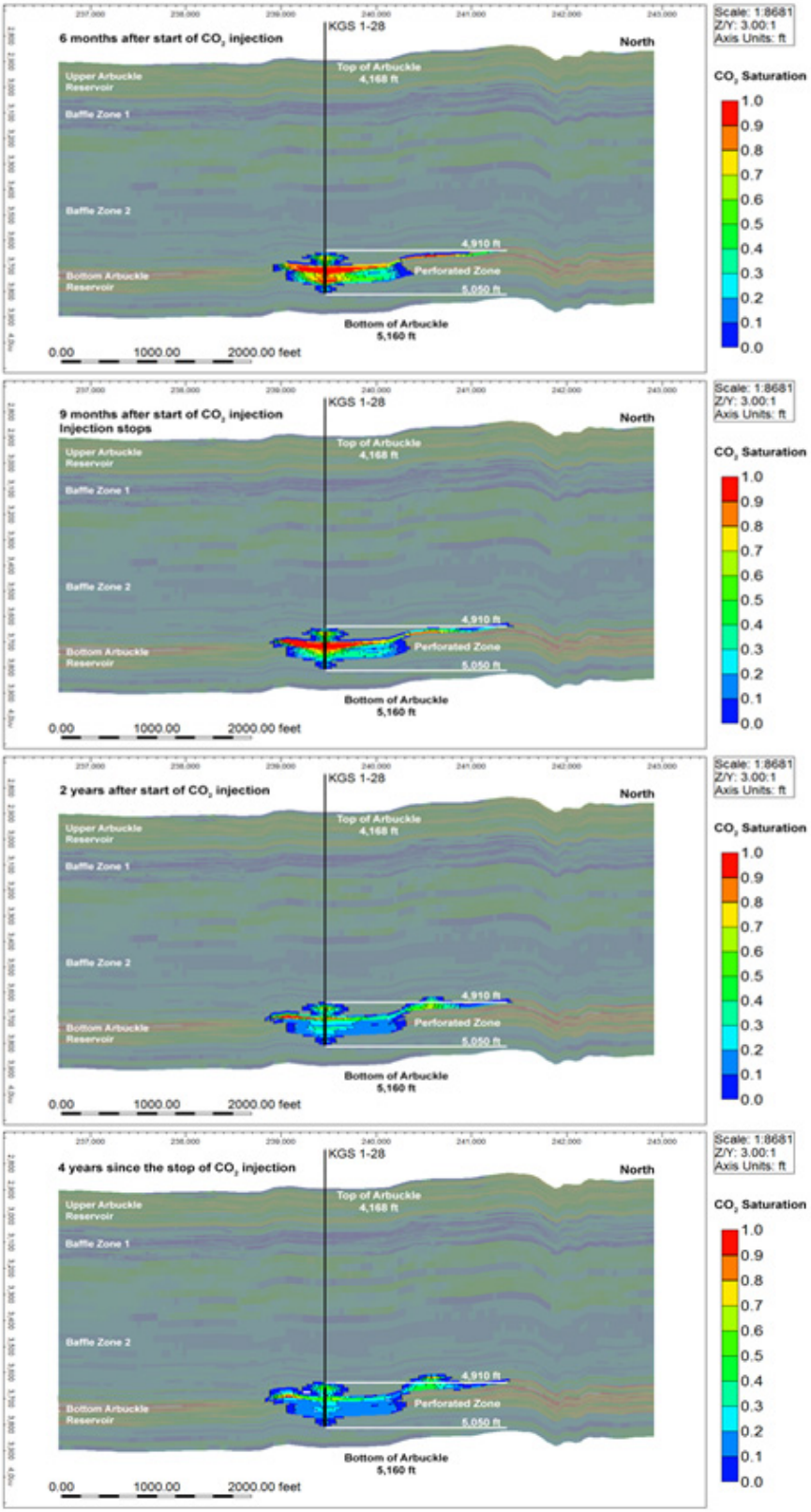

Figure 22. N-S cross section showing vertical and lateral separate-phase plume migration at selected operational milestones for the 26,000 MT scenario.

The distribution of CO_2 phases (supercritical, trapped, and dissolved) for this scenario is presented in Figure 23. As discussed above, the AoR was defined based on the maximum extent of the separate-phase plume, following EPA guidance.

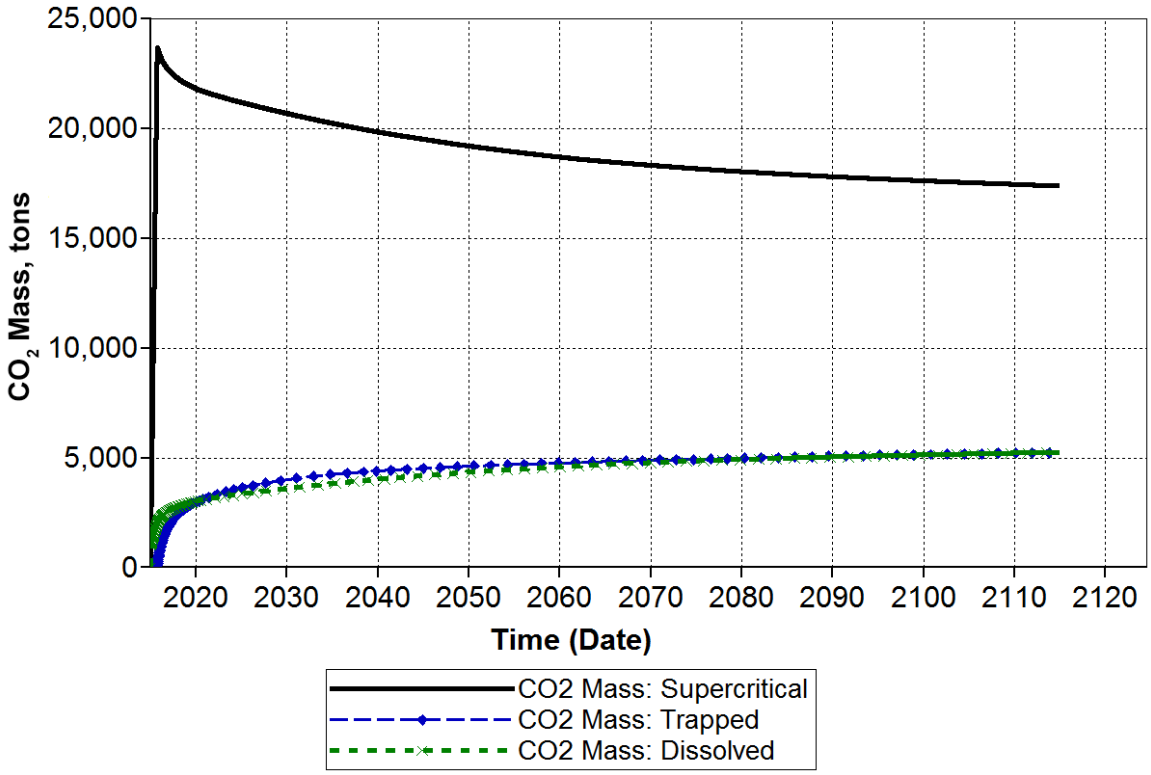

Figure 23. Mass partitioning in the model domain over time showing the change in integrated CO_2 mass in the gas, dissolved, and trapped phases for the 26,000 MT scenario.

The maximum bottomhole pressure occurs under the low porosity/low permeability model scenario (k-0.75/phi-0.75). Pressure decreases rapidly with distance from the injection well (Figure 24). The confining effect of the low-permeability baffle zone in the mid-Arbuckle prevents pressure increases in the vertical direction. The large pressure increases as a result of injection are mostly restricted to the injection interval (lower Arbuckle).

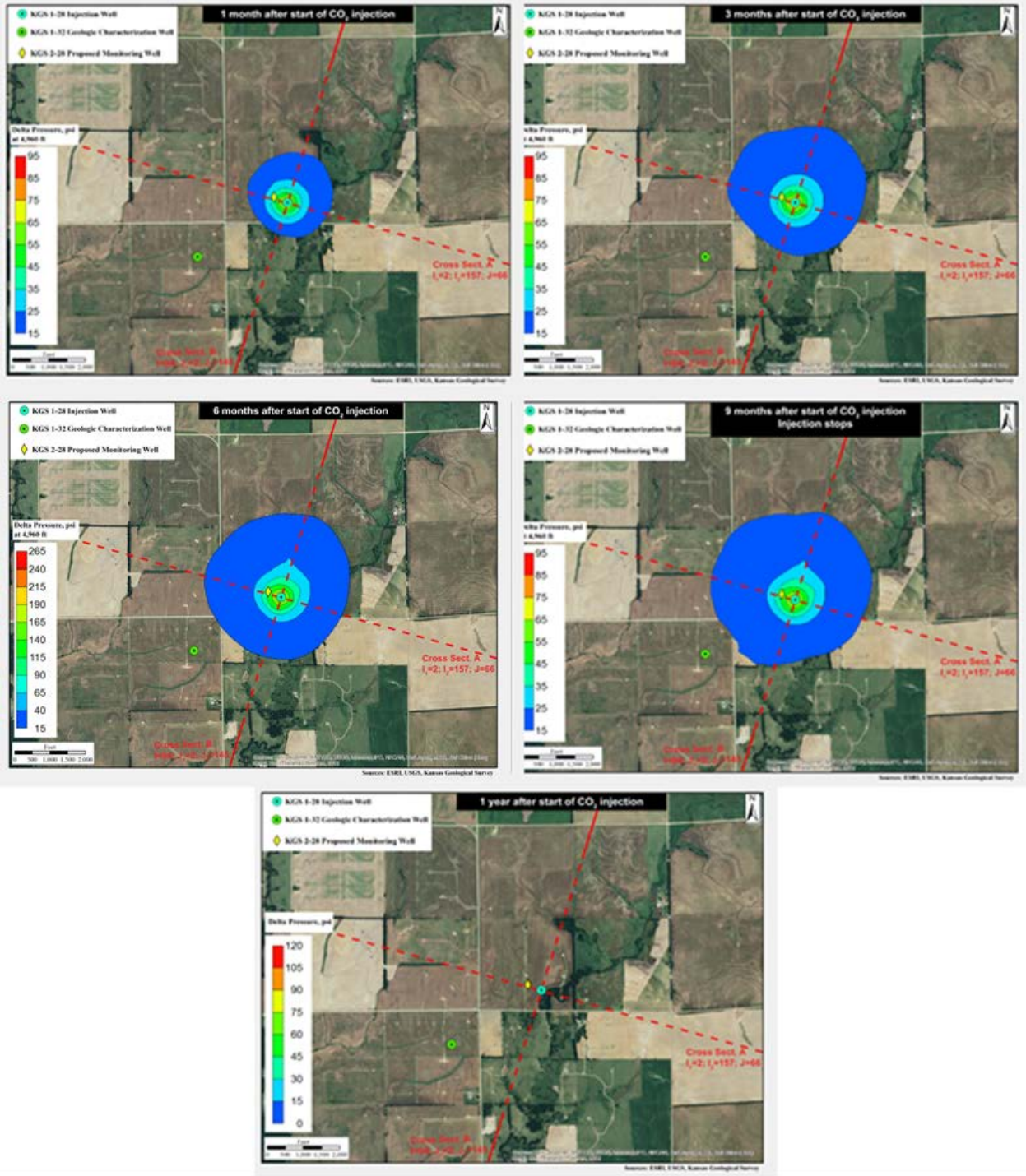

Figure 24. Evolution of the pressure front over time for the 26,000 MT scenario.

Bottomhole pressure increases to 2,361 psi when injection starts and drops significantly when injection ceases (Figure 25). This is a pressure increase of 268 psi over the pre-injection levels, with a resulting pressure gradient of 0.467 psi/ft, which is less than the maximum allowable pressure gradient of 0.525 psi/ft corresponding to 70% of the fracture gradient. In terms of lateral distribution, pressure increases from commencement of injection to nine months (end of injection) and then drops significantly by the end of the first year after cessation of injection.

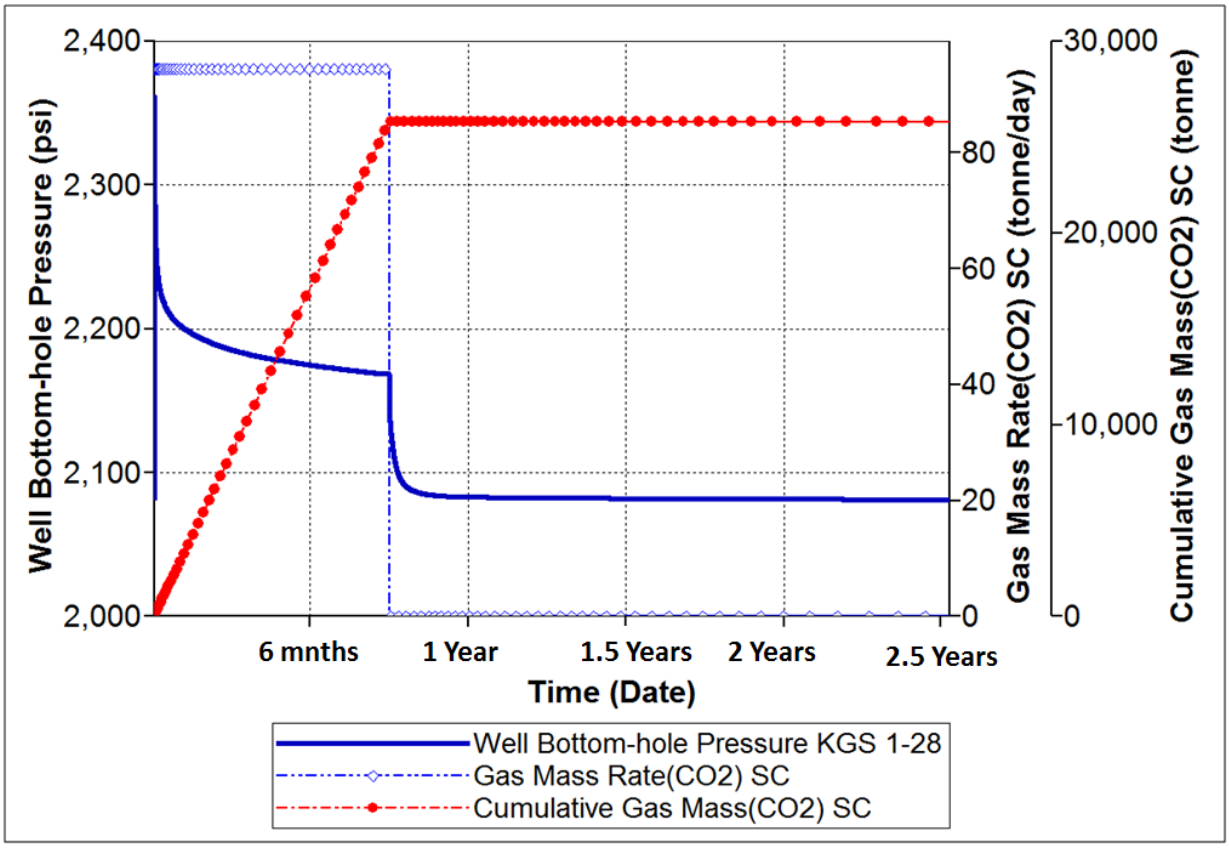

Figure 25. Maximum bottomhole pressure for the 26,000 MT scenario at a depth of 5,050 feet for the minimum porosity and minimum permeability scenario (k-0.75/phi-0.75).

An increase in pore pressure at KGS 2-28 is expected within seconds from the start of CO_2 injection with an eventual maximum projected change in pressure of approximately 40 psi. The pressure is projected to fall to ambient levels within two to three months after CO_2 injection has ceased.

Model Calibration and Validation

To support a request for an alternative PISC timeframe, Berexco conducted sensitivity analyses pursuant to 40 CFR 146.93(c)(2)(vi) to identify and assess parameters that contribute significantly to uncertainty. Non-isothermal sensitivity analyses were conducted to demonstrate that including temperature as a variable only minimally impacts the plume extent and pressure distribution. The effects of water salinity on the simulated AoR were found to be negligible (less

than 5%), justifying the use of uniform salinity concentrations during AoR modeling. Sensitivity runs were performed with dispersion and diffusion to demonstrate the impact of these parameters, which result in a 5% difference in the extent of the AoR. To analyze the influence of boundary conditions, a closed boundary was compared to the Carter-Tracy boundary; results indicated that the increase in pore pressures and the plume extent were not meaningfully different when using a closed boundary.

As discussed above in the context of the AoR modeling results, a suite of permeability and porosity alternative models were evaluated. The base-case reservoir model was carefully constructed using the Petrel geomodel, using site-specific hydrogeologic information obtained from laboratory tests and log-based analyses. To account and test for the sensitivity of hydrogeologic uncertainties, a set of alternative parametric models were developed by varying the porosity and horizontal hydraulic permeability by 25% (positive and negative). The maximum plume extent and pressure distributions were determined based on the "worst-case" scenario from this suite of alternative models.

AoR Delineation

EPA recommends that a Class VI AoR be delineated based on the maximum extent of the either the separate-phase plume or the pressure front (USEPA, 2011). The goal is to define the extent of the plume and pressure front within which any artificial or natural penetration could have the potential to allow fluids from the injection to endanger a USDW. Critical pressure and estimated bottomhole pressure were calculated to investigate the potential impact of the pressure front, and results indicated a large difference between expected bottomhole and critical pressure. Due to this and a number of other factors, including the lack of a USDW in the AoR, the AoR was defined based on the CO_2 plume and not the pressure front.

The plume-based AoR is defined by the boundary that encompasses the injected free-phase CO_2 with a concentration greater than 0.5%. As discussed earlier in this plan, the maximum plume extent results from the alternative permeability/porosity model with the largest permeability and lowest porosity (K-1.25/phi-0.75). The plume-based AoR was derived from the maximum 40,000 MT injection scenario, which provides a conservative estimate of plume extent considering that the expected injection amount will be 26,000 MT. Figure 26 shows the AoR drawn around the maximum plume extent at the end of the model period (100 years).

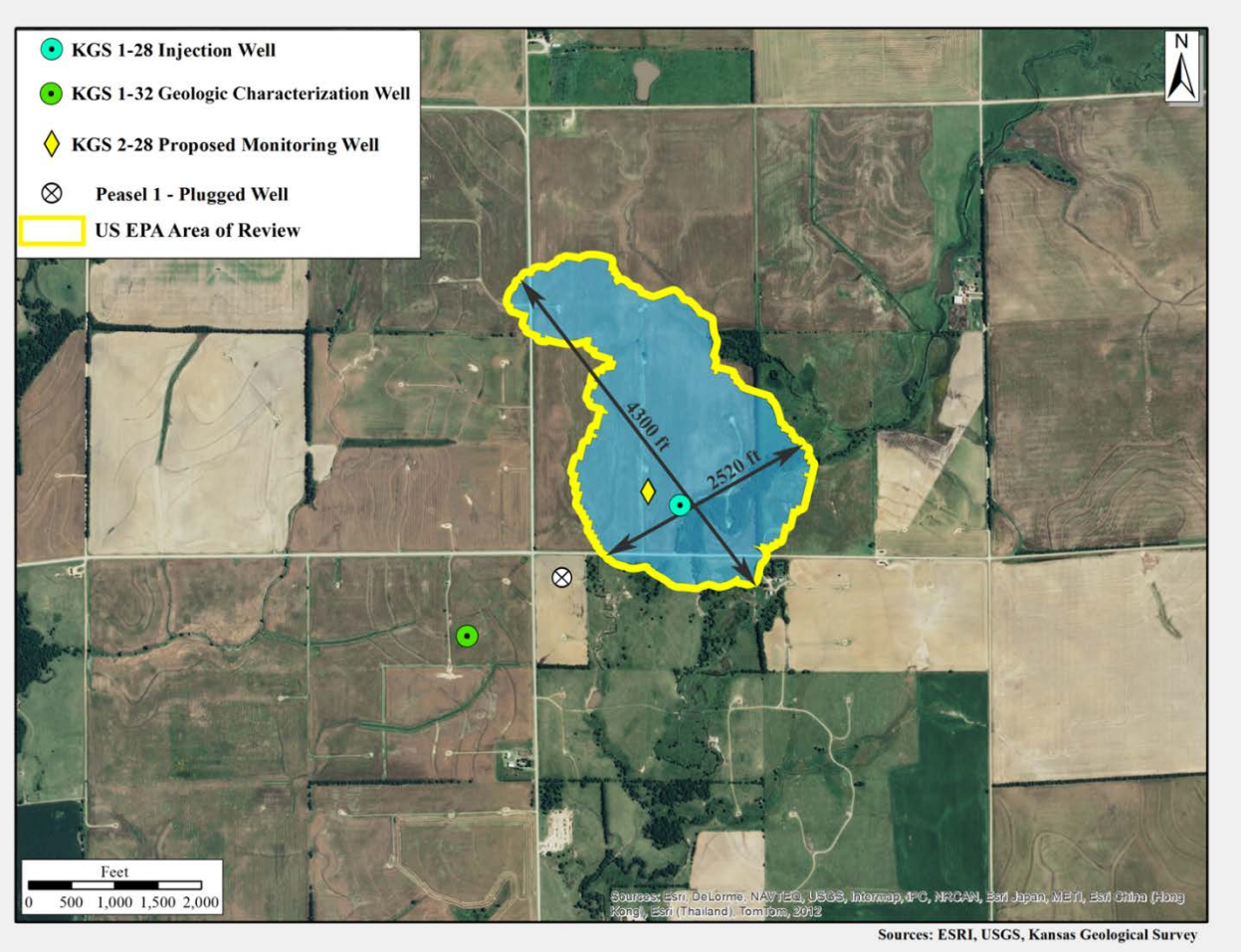

Figure 26. Separate-phase CO_2 plume at the end of the 100-year model period under the 40,000 MT scenario, used to delineate the AoR (in yellow).

Corrective Action

Tabulation of Wells within the AoR

Wells within the AoR

Figure 27 shows the locations of wells within the AoR.

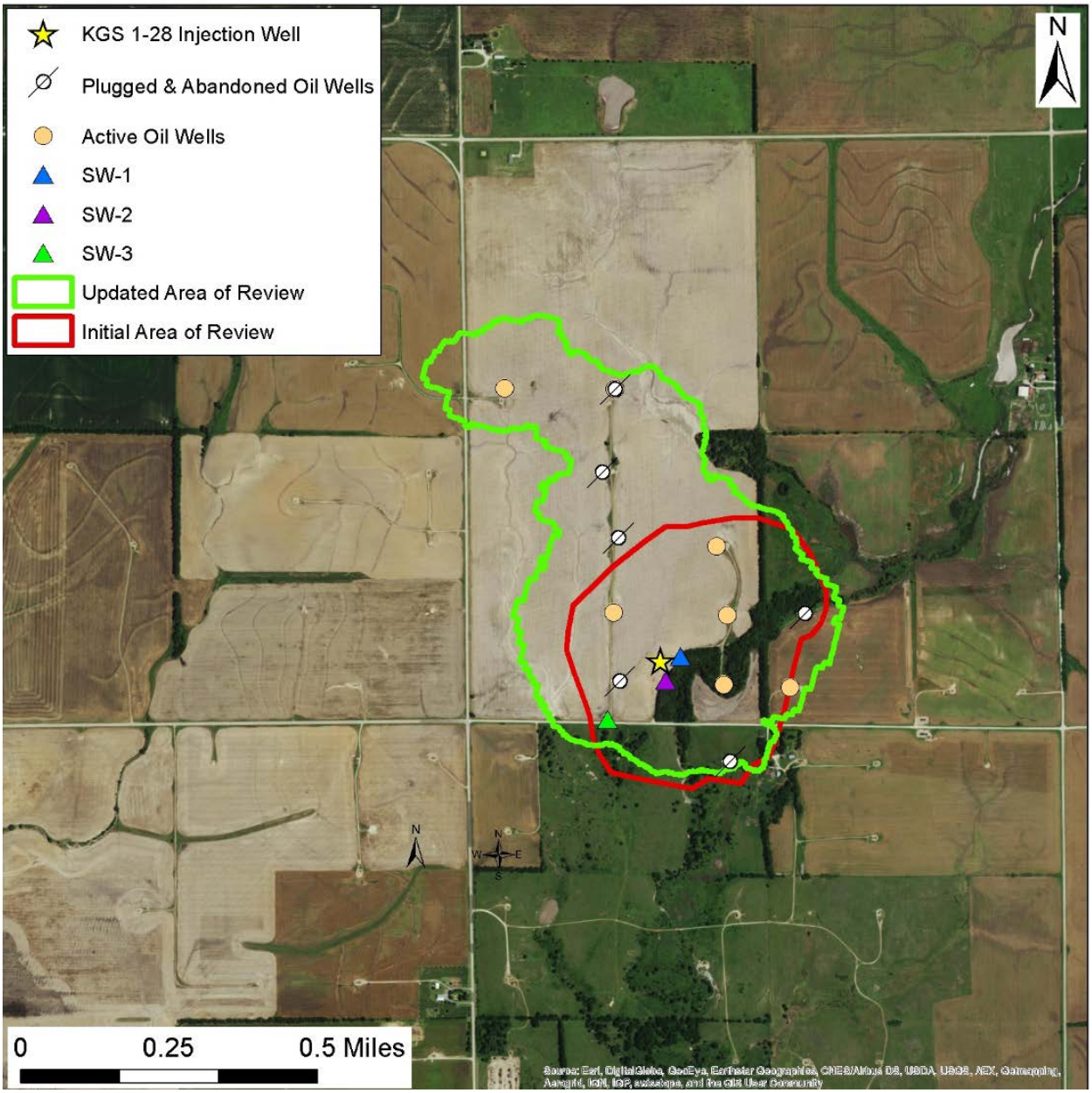

Figure 27. Wells within the AoR, as identified by Berexco in December 2015.

Table 8 presents key details about the identified wells within the AoR. As shown in the table, these wells include:

- Three shallow monitoring wells to be used for monitoring water quality above the confining zone (SW-1, SW-2, and SW-3);
- Twelve production or injection wells (five active wells and seven inactive wells, including wells coded as "plugged and abandoned," "inactive," and "authorized" in the state well records database); and
- The Arbuckle CO_2 injection well (KGS 1-28).

Table 8. Wells within the AoR, as identified by Berexco in December 2015. The injection well, KGS 1-28, is shown in *bold italic* type.

Well Name/Number	10-Digit API Number	Depth (ft)	Status	Type
Wellington Unit 32	15-191-10045	3,678	Active	Oil
Wellington Unit 139-INJ	15-191-10046	3,683	Authorized	Injection/EOR
Wellington Unit 2	15-191-10047	3,674	Plugged and Abandoned	Oil
Wellington Unit 13	15-191-10049	3,698	Active	Oil
Wellington Unit 31-INJ	15-191-10051	3,704	Plugged and Abandoned	Injection/EOR
Wellington Unit 15-INJ	15-191-10052	3,683	Inactive	Injection/EOR
Wellington Unit 20-INJ	15-191-10053	1,271	Authorized	Injection/EOR
Wellington Unit 25	15-191-10054	3,681	Active	Oil
Wellington Unit 24	15-191-10055	3,707	Active	Oil
Wellington Unit 37	15-191-19006	3,671	Plugged and Abandoned	Oil
Wellington Unit 137-INJ	15-191-19022	3,705	Plugged and Abandoned	Injection/EOR
Wellington Unit 1-28	***15-191-22590***	***5,250***	***Inactive***	***Other***
Wellington Unit 143-INJ	15-191-43782	3,708	Active	Injection/EOR
SW-1	N/A	50	N/A	Monitoring
SW-2	N/A	100	N/A	Monitoring
SW-3	N/A	200	N/A	Monitoring

Wells Penetrating the Confining Zone

The only well in the AoR that penetrates the confining zone is the (proposed) injection well (KGS 1-28); the Arbuckle monitoring well (KGS 2-28; to be constructed) will also penetrate the confining zone. The geologic characterization well (KGS 1-32) is outside of the delineated AoR. Because the injection and monitoring wells are or will be constructed in accordance with 40 CFR 146.86, no corrective action needs have been identified for wells within the AoR. Construction details for the injection well are provided in Attachment G to the Class VI permit.

Plan for Site Access

The Wellington site is in close proximity to paved roads in the area, thereby providing easy access. Berexco is the operator of the Wellington oil field and has permission to access all well sites should that be necessary to perform any corrective action.

Corrective Action Schedule

As discussed earlier, because the Arbuckle wells within the AoR either were constructed (KGS 1-28) or will be constructed (KGS 2-28) in accordance with 40 CFR 146.86, no corrective action is presently required. Should future modeling (i.e., associated with an AoR reevaluation, as discussed below) indicate that the AoR extends beyond the present AoR boundary and includes additional wells that penetrate the confining zone, the Corrective Action component of this plan will be revised to include the well name, location, planned date of corrective action, planned corrective action method, and any other pertinent information required by the UIC Program Director. If the result of an AoR reevaluation indicate corrective action is required, it will be implemented as expeditiously as possible in consultation with the EPA.

AoR Reevaluation Schedule and Criteria

The AoR reevaluation will ensure that site monitoring data are used to update modeling results and that the AoR delineation reflects any substantial changes in operational conditions. Berexco will take the following steps to evaluate project data and, if necessary, reevaluate the AoR. AoR reevaluations will be performed during the injection and post-injection phases. Specifically, Berexco will:

- Review available monitoring data and compare it to the model predictions. Berexco will analyze monitoring and operational data from the injection well (KGS 1-28), the monitoring wells, and other sources specified in the Testing and Monitoring Plan (Attachment C to this permit) and the Post-Injection Site Care and Site Closure Plan (Attachment E to this permit), to assess whether the predicted CO_2 plume migration is consistent with actual data. Specific steps of this review include:
    - Reviewing available data on the position of the CO_2 plume and pressure front (including pressure and temperature monitoring data and RST saturation and seismic survey data). Specific activities will include:
        - Correlating data from geophysical monitoring techniques and other methods to locate and track the movement of the CO_2 plume. A good correlation between the data sets will provide strong evidence in validating the model's ability to represent the storage system.
        - Reviewing reservoir pressure data collected from various locations and intervals using a combination of surface and downhole pressure gauges.
    - Reviewing ground water chemistry monitoring data taken in the shallow and deep monitoring wells above the confining zone to verify that there is no evidence of excursion of carbon dioxide or brines that represent an endangerment to any USDWs.
    - Reviewing operating data, e.g., on injection rates, the mass of CO_2 injected, the injection period, and pressures, and verifying that it is consistent with the inputs used in the most recent modeling effort.

- Reviewing any geologic data acquired since the last modeling effort, including any additional site characterization performed (e.g., in the course of nearby oilfield activities), updates of petrophysical properties from core analysis, etc., and identifying whether any new data materially differ from modeling inputs/assumptions. This information may include, but is not limited to, data on carbonate precipitation or new information on faults near the project (including the fault to the west of the well).

- Compare the results of computational modeling used for AoR delineation to monitoring data collected. Monitoring data will be used to show that the computational model accurately represents the storage site and can be used as a proxy to determine the plume's properties and size. Berexco will demonstrate this degree of accuracy by comparing monitoring data against the model's predicted properties (i.e., plume location, rate of movement/arrival time at the Arbuckle monitoring well, and pressure decay). Statistical methods will be employed to correlate the data and confirm the model's ability to accurately represent the storage site.

- If the information reviewed is consistent with, or is unchanged from, the most recent modeling assumptions or confirms modeled predictions about the maximum extent of plume and pressure front movement, Berexco will prepare a report demonstrating that, based on the monitoring and operating data, no reevaluation of the AoR is needed. The report will include the data and results demonstrating that no changes are necessary.

- If material changes have occurred (e.g., in the behavior of the plume and pressure front, operations, or site conditions) such that the actual plume or pressure front may extend beyond the modeled plume and pressure front, Berexco will re-delineate the AoR, as required at 40 CFR 146.84(e). The following steps will be taken, as necessary:

    - Revising the site conceptual model based on new site characterization, operational, or monitoring data.

    - Calibrating the model in order to minimize the differences between monitoring data and model simulations.

    - Performing the AoR delineation as described the Computational Modeling Section of this AoR and Corrective Action Plan (and documenting any modeling approaches or procedures that have changed since the previous AoR delineation).

- Review wells in any newly identified areas of the AoR and apply corrective action to any deficient wells. Specific steps include:

    - Identifying any new wells within the AoR that penetrate the confining zone and provide a description of each well's type, construction, date drilled, location, depth, record of plugging and/or completion.

    - Determining which abandoned wells in the newly delineated AoR have been plugged in a manner that prevents the movement of carbon dioxide or other fluids that may endanger USDWs.

    - Performing corrective action on all deficient wells in the AoR using methods designed to prevent the movement of fluid into or between USDWs, including the use of materials compatible with carbon dioxide.

- Prepare a report documenting the AoR reevaluation process, data evaluated, any corrective actions determined to be necessary, and the status of corrective action or a schedule for any corrective actions to be performed. The report will include maps that highlight similarities and differences in comparison with previous AoR delineations. The report will be submitted to EPA within six (6) months of the reevaluation; for the scheduled reevaluation that will take place at the end of the post-injection phase (see below), the results of the reevaluation will be incorporated into the non-endangerment demonstration in lieu of a separate report.
- Update this AoR and Corrective Action Plan to reflect the revised AoR, along with other related project plans, as needed.

AoR Reevaluation Cycle

Berexco will reevaluate the above-described AoR at the end of the injection phase. The alternative PISC timeframe for this project is four years following the cessation of injection. Therefore, the 5-year reevaluation requirement at 40 CFR 146.84(e) will apply at the end of the post-injection phase. Following the AoR reevaluation at the end of the PISC period, Berexco will submit the results of the AoR reevaluation as part of their non-endangerment demonstration (see Attachment E). If non-endangerment cannot be demonstrated/site closure is not authorized, Berexco will update and submit the AoR and Corrective Action Plan as described above.

Factors that may trigger an unscheduled AoR reevaluation are described in detail below.

Triggers for AoR Reevaluations Prior to the Next Scheduled Reevaluation

Unscheduled reevaluations of the AoR will be based on quantitative changes in operational parameters (from those described in Attachment A of the permit) or based on the results of ground water or plume and pressure front monitoring, as performed pursuant to the Testing and Monitoring Plan (Attachment C) or the PISC and Site Closure Plan (Attachment E) wells. These changes include:

1. If the bottomhole pressure exceeds 70% of the fracture gradient (0.75 psi/ft).
2. If newly-collected characterization data at KGS 2-28 (monitoring well) are deemed to significantly alter the hydrogeologic properties specified in the reservoir model.
3. If the arrival time of the plume and/or pressure front at the deep monitoring well (KGS 2-28) and/or when pressure and plume data recorded at KGS 2-28 differs significantly from model projections. Reevaluation based on arrival time at KGS 2-28 will be conducted at the direction of EPA Region 7.
4. At the termination of injection.
5. Prior to site closure to demonstrate the stability of the plume and pressure front, given the alternative PISC timeframe.
6. If the following events occur and reevaluation is determined to be warranted based on evaluation of the event impact:

a. Change in modeled direction of plume movement or vertical and lateral plume distribution as detected by means other than the monitoring well, KGS 2-28 (evaluation within one month of detection);

b. Initiation of competing Arbuckle injection projects within the same injection formation within a 1-mile radius of the injection well (evaluation within one month of initiation);

c. A significant deviation of monitored wellhead operational data, or formation pressure and plume migration data;

d. Significant land-use changes that would impact site access (evaluation within one month of identification);

e. New site characterization data that identifies additional faults within the AoR (evaluation within one month of identification);

f. Seismic events or other emergency events that trigger an AoR reevaluation as specified in the Emergency and Remedial Response Plan (Attachment F of the permit);

g. Any other activity prompting a model recalibration.

Berexco will discuss any such events with the UIC Program Director to determine if an AoR reevaluation is required. If an unscheduled reevaluation is triggered, Berexco will perform the steps described above.

Appendix 1. Relative permeability and capillary pressure data submitted to EPA.

(S_l is aqueous saturation, S_g is CO_2 saturation, K_{rl} is aqueous relative permeability, K_{rg} is gas relative permeability, and P_c is capillary pressure)

Drainage					Imbibition				
Rock Type 1 (RQI range from 10-40)					Rock Type 1 (RQI range from 10-40)				
P_c	S_l	S_g	K_{rl}	k_{rg}	P_c	S_l	S_g	K_{rl}	k_{rg}
0	1	0	1	0	0	0.652	0.348	0.075032	0.0000
0.012	0.933	0.0666	0.8758	0.0000	0.005	0.4689	0.5311	0.027558	0.0184
0.015	0.765	0.2348	0.5973	0.0011	0.01	0.3693	0.6307	0.013298	0.0650
0.018	0.651	0.3494	0.4368	0.0065	0.02	0.2627	0.7373	0.004674	0.1645
0.02	0.593	0.4075	0.3646	0.0129	0.03	0.2060	0.7940	0.002204	0.2440
0.03	0.414	0.5862	0.1818	0.0664	0.04	0.1706	0.8294	0.001225	0.3045
0.04	0.321	0.6789	0.1110	0.1285	0.05	0.1463	0.8537	0.000756	0.3512
0.05	0.264	0.7360	0.0757	0.1848	0.06	0.1285	0.8715	0.000502	0.3882
0.06	0.225	0.7748	0.0553	0.2329	0.07	0.1150	0.8850	0.000352	0.4181
0.07	0.197	0.8031	0.0425	0.2736	0.08	0.1042	0.8958	0.000257	0.4428
0.08	0.175	0.8246	0.0338	0.3081	0.09	0.0955	0.9045	0.000194	0.4635
0.09	0.158	0.8415	0.0276	0.3377	0.1	0.0883	0.9117	0.00015	0.4812
0.1	0.145	0.8552	0.0230	0.3631	0.2	0.0525	0.9475	2.64E-05	0.5751
0.15	0.103	0.8974	0.0115	0.4509	0.3	0.0391	0.9609	9.21E-06	0.6135
0.2	0.081	0.9192	0.0070	0.5024	0.4	0.0319	0.9681	4.31E-06	0.6345
0.3	0.058	0.9418	0.0035	0.5605	0.5	0.0274	0.9726	2.38E-06	0.6479
0.4	0.046	0.9535	0.0021	0.5926	0.6	0.0243	0.9757	1.46E-06	0.6572
0.5	0.039	0.9608	0.0014	0.6131	0.7	0.0221	0.9779	9.6E-07	0.6641
0.6	0.034	0.9657	0.0010	0.6273	0.8	0.0204	0.9796	6.68E-07	0.6693
0.7	0.031	0.9693	0.0008	0.6379	0.9	0.0190	0.9810	4.84E-07	0.6735
0.8	0.028	0.9720	0.0006	0.6459	1	0.0179	0.9821	3.63E-07	0.6769
0.9	0.026	0.9741	0.0005	0.6524	2	0.0127	0.9873	5.25E-08	0.6931
1	0.024	0.9759	0.0004	0.6576	3	0.0109	0.9891	1.64E-08	0.6989
1.5	0.019	0.9812	0.0002	0.6740	4	0.0099	0.9901	6.99E-09	0.7019
2	0.016	0.9840	0.0001	0.6825	5	0.0093	0.9907	3.55E-09	0.7038
3	0.013	0.9868	0.0001	0.6915	6	0.0089	0.9911	2.01E-09	0.7051
4	0.012	0.9883	3.62E-05	0.6962	7	0.0086	0.9914	1.23E-09	0.7060
5	0.011	0.9892	2.40E-05	0.6991	8	0.0084	0.9916	7.91E-10	0.7067
6	0.010	0.9898	1.70E-05	0.7011	9	0.0082	0.9918	5.31E-10	0.7073
7	0.010	0.9903	1.27E-05	0.7025	10	0.0081	0.9919	3.68E-10	0.7077
8	0.009	0.9906	9.76E-06	0.7036	12	0.0079	0.9921	1.9E-10	0.7084
9	0.009	0.9909	7.73E-06	0.7045	14	0.0077	0.9923	1.05E-10	0.7089
10	0.009	0.9911	6.26E-06	0.7052	20	0.0074	0.9926	0	0.7112
12	0.009	0.9915	4.30E-06	0.7063	30	0.0072	0.9928	0	0.7112
14	0.008	0.9917	3.10E-06	0.7071	40	0.0071	0.9929	0	0.7112
18	0.008	0.9920	1.77E-06	0.7081	50	0.0070	0.9930	0	0.7112

Drainage					Imbibition				
Rock Type 1 (RQI range from 10-40)					Rock Type 1 (RQI range from 10-40)				
P_c	S_l	S_g	K_{rl}	k_{rg}	P_c	S_l	S_g	K_{rl}	k_{rg}
20	0.008	0.9922	1.38E-06	0.7085	60	0.0069	0.9931	0	0.7112
25	0.008	0.9924	7.86E-07	0.7092	70	0.0069	0.9931	0	0.7112
30	0.007	0.9925	4.75E-07	0.7097	80	0.0069	0.9931	0	0.7112
40	0.007	0.9927	1.87E-07	0.7103	90	0.0069	0.9931	0	0.7112
50	0.007	0.00	0.00	0.7112	100	0.0068	0.9932	0	0.7112
60	0.007	0.00	0.00	0.7112	150	0.0068	0.9932	0	0.7112
70	0.007	0.00	0.00	0.7112	200	0.0068	0.9932	0	0.7112
80	0.007	0.00	0.00	0.7112	300	0.0067	0.9933	0	0.7112
90	0.007	0.00	0.00	0.7112					
100	0.007	0.00	0.00	0.7112					
150	0.007	0.00	0.00	0.7112					
200	0.007	0.00	0.00	0.7112					
300	0.007	0.00	0.00	0.7112					

Drainage					Imbibition				
Rock Type 2 (RQI range from 2.5-10)					Rock Type 2 (RQI range from 2.5-10)				
P_c	S_l	S_g	K_{rl}	k_{rg}	P_c	S_l	S_g	K_{rl}	k_{rg}
0	1.000	0	1	0	0	0.652	0.348	0.121501	0
0.06	0.954	0.046311	0.911705	1.19E-06	0.005	0.606	0.3943	0.0967	0.0005
0.07	0.833	0.167467	0.699192	0.000318	0.01	0.566	0.4341	0.0783	0.0026
0.08	0.740	0.259685	0.555519	0.002142	0.02	0.501	0.4987	0.0537	0.0125
0.09	0.668	0.33234	0.453456	0.006265	0.03	0.451	0.5492	0.0385	0.0281
0.1	0.609	0.391133	0.378118	0.012725	0.04	0.410	0.5897	0.0286	0.0469
0.15	0.428	0.571954	0.187715	0.066459	0.05	0.377	0.6229	0.0219	0.0673
0.2	0.334	0.665688	0.114064	0.128606	0.06	0.349	0.6508	0.0172	0.0881
0.3	0.237	0.762741	0.056377	0.232473	0.07	0.326	0.6744	0.0137	0.1088
0.4	0.187	0.813051	0.03411	0.306934	0.08	0.305	0.6948	0.0112	0.1289
0.5	0.156	0.844044	0.023058	0.361178	0.09	0.287	0.7125	0.0092	0.1482
0.6	0.135	0.865142	0.016719	0.402126	0.1	0.272	0.7281	0.0077	0.1666
0.7	0.120	0.880474	0.012724	0.434061	0.2	0.180	0.8196	0.0020	0.3047
0.8	0.108	0.892145	0.010033	0.459649	0.3	0.138	0.8615	0.0008	0.3868
0.9	0.099	0.901339	0.008128	0.480615	0.4	0.114	0.8859	0.0004	0.4403
1	0.091	0.90878	0.006727	0.498113	0.5	0.098	0.9018	0.0002	0.4778
1.5	0.068	0.931663	0.003218	0.555021	0.6	0.087	0.9131	0.0001	0.5056
2	0.056	0.943525	0.001885	0.586423	0.7	0.078	0.9215	0.0001	0.5270
3	0.044	0.955808	0.000866	0.620361	0.8	0.072	0.9281	0.0001	0.5441
4	0.038	0.962174	0.000487	0.638539	0.9	0.067	0.9334	0.0000	0.5580
5	0.034	0.966097	0.000305	0.649939	1	0.062	0.9377	0.0000	0.5696
6	0.031	0.968767	0.000204	0.657789	2	0.042	0.9584	0.0000	0.6275

Drainage					Imbibition				
Rock Type 2 (RQI range from 2.5-10)					Rock Type 2 (RQI range from 2.5-10)				
P_c	S_l	S_g	K_{rl}	k_{rg}	P_c	S_l	S_g	K_{rl}	k_{rg}
7	0.029	0.970707	0.000144	0.663539	3	0.034	0.9660	0.0000	0.6496
8	0.028	0.972184	0.000104	0.667942	4	0.030	0.9700	0.0000	0.6614
9	0.027	0.973348	7.73E-05	0.671427	5	0.028	0.9725	0.0000	0.6688
10	0.026	0.974289	5.84E-05	0.674257	6	0.026	0.9742	0.0000	0.6739
12	0.024	0.975722	3.45E-05	0.678581	7	0.025	0.9754	0.0000	0.6776
14	0.023	0.976764	2.09E-05	0.681738	8	0.024	0.9763	0.0000	0.6804
18	0.022	0.978181	7.69E-06	0.686051	9	0.023	0.9771	0.0000	0.6827
20	0.021	0.978686	4.49E-06	0.687594	10	0.022	0.9777	0.0000	0.6845
25	0.020	0.979611	7.99E-07	0.690425	12	0.021	0.9786	0.0000	0.6873
30	0.020	0.980241	0	0.692357	14	0.021	0.9793	0.0000	0.6894
40	0.019	0.981	0	0.692357	20	0.020	0.981	0	0.6924
50	0.018	0.982	0	0.692357	30	0.0185	0.9815	0	0.6924
60	0.018	0.982	0	0.692357	40	0.0180	0.9820	0	0.6924
70	0.018	0.982	0	0.692357	50	0.0177	0.9823	0	0.6924
80	0.018	0.982	0	0.692357	60	0.0174	0.9826	0	0.6924
90	0.018	0.982	0	0.692357	70	0.0173	0.9827	0	0.6924
100	0.017	0.983	0	0.692357	80	0.0172	0.9828	0	0.6924
150	0.017	0.983	0	0.692357	90	0.0171	0.9829	0	0.6924
200	0.017	0.983	0	0.692357	100	0.0170	0.9830	0	0.6924
300	0.017	0.983	0	0.692357	150	0.0168	0.9832	0	0.6924
					200	0.0166	0.9834	0	0.6924
					300	0.0165	0.9835	0	0.6924

Drainage					Imbibition				
Rock Type 3 (RQI range from 1-2.5)					Rock Type 3 (RQI range from 1-2.5)				
P_c	S_l	S_g	K_{rl}	k_{rg}	P_c	S_l	S_g	K_{rl}	k_{rg}
0	1.000	0	1	0	0	0.654	0.346	0.189511	0
0.3	0.868	0.131574	0.752199	0.000167	0.005	0.643	0.356679	0.179635	1.18E-05
0.4	0.679	0.320874	0.45511	0.007077	0.01	0.633	0.366974	0.170445	7.54E-05
0.5	0.563	0.437491	0.307641	0.026021	0.02	0.614	0.386496	0.153889	0.000452
0.6	0.483	0.516876	0.223065	0.052417	0.03	0.595	0.404715	0.139439	0.001237
0.7	0.425	0.574567	0.169764	0.081749	0.04	0.578	0.421759	0.126767	0.002468
0.8	0.382	0.618479	0.13386	0.111382	0.05	0.562	0.437739	0.115606	0.004143
0.9	0.347	0.653076	0.108447	0.13999	0.06	0.547	0.452754	0.105734	0.006245
1	0.319	0.681071	0.089755	0.166978	0.07	0.533	0.46689	0.09697	0.008742
1.5	0.233	0.767174	0.042942	0.275299	0.08	0.520	0.480224	0.08916	0.011601
2	0.188	0.811808	0.025156	0.349104	0.09	0.507	0.492822	0.082176	0.014787
3	0.142	0.858022	0.011556	0.440498	0.1	0.495	0.504746	0.075912	0.018263
4	0.118	0.881978	0.006492	0.494509	0.2	0.404	0.596381	0.038024	0.062589

Drainage					Imbibition				
Rock Type 3 (RQI range from 1-2.5)					Rock Type 3 (RQI range from 1-2.5)				
P_c	S_l	S_g	K_{rl}	k_{rg}	P_c	S_l	S_g	K_{rl}	k_{rg}
5	0.103	0.896736	0.004068	0.530205	0.3	0.344	0.656344	0.021774	0.111804
6	0.093	0.906783	0.002728	0.555603	0.4	0.301	0.698778	0.013632	0.158065
7	0.086	0.914084	0.001915	0.574635	0.5	0.270	0.730464	0.009096	0.199413
8	0.080	0.919641	0.001388	0.589451	0.6	0.245	0.755069	0.006367	0.235796
9	0.076	0.924019	0.001031	0.601328	0.7	0.225	0.774756	0.004626	0.267721
10	0.072	0.927562	0.000779	0.611071	0.8	0.209	0.790883	0.003463	0.295801
12	0.067	0.932954	0.00046	0.62613	0.9	0.196	0.804346	0.002656	0.32061
14	0.063	0.936873	0.000279	0.63725	1	0.184	0.815765	0.002079	0.342646
18	0.058	0.942205	0.000103	0.652624	2	0.124	0.876117	0.000346	0.474936
20	0.056	0.944107	5.99E-05	0.658174	3	0.099	0.900586	0.000104	0.5365
25	0.052	0.947587	1.07E-05	0.668423	4	0.086	0.913988	4E-05	0.572243
30	0.050	0.949955	0	0.675469	5	0.078	0.922497	1.78E-05	0.595694
40	0.047	0.050045	0	0.675469	6	0.072	0.928401	8.61E-06	0.612315
50	0.045	0.949955	0	0.675469	7	0.067	0.932748	4.38E-06	0.62474
60	0.044	0.050045	0	0.675469	8	0.064	0.93609	2.29E-06	0.634396
70	0.043	0.949955	0	0.675469	9	0.061	0.938742	1.21E-06	0.642127
80	0.042	0.050045	0	0.675469	10	0.059	0.940901	6.39E-07	0.648464
90	0.042	0.949955	0	0.675469	12	0.056	0.944208	1.63E-07	0.658247
100	0.041	0.050045	0	0.675469	14	0.053	0.946628	3.17E-08	0.665464
150	0.040	0.949955	0	0.675469	20	0.0489	0.9511	0	0.675469
200	0.039	0.050045	0	0.675469	30	0.0452	0.9548	0	0.675469
300	0.038	0.949955	0	0.675469	40	0.0433	0.9567	0	0.675469
					50	0.0421	0.9579	0	0.675469
					60	0.0413	0.9587	0	0.675469
					70	0.0407	0.9593	0	0.675469
					80	0.0403	0.9597	0	0.675469
					90	0.0399	0.9601	0	0.675469
					100	0.0396	0.9604	0	0.675469
					150	0.0387	0.9613	0	0.675469
					200	0.0383	0.9617	0	0.675469
					300	0.0378	0.9622	0	0.675469

Drainage					Imbibition				
Rock Type 4 (RQI range from 0.5-1)					Rock Type 4 (RQI range from 0.5-1)				
P_c	S_l	S_g	K_{rl}	k_{rg}	P_c	S_l	S_g	K_{rl}	k_{rg}
0	1.000	0	1	0	0	0.657	0.3426	0.254272	0
0.7	0.989	0.010684	0.977573	1.03E-08	0.005	0.653	0.34683	0.248578	1.95E-06
0.8	0.885	0.115298	0.770825	0.000158	0.01	0.649	0.350608	0.243564	1.04E-05
0.9	0.802	0.19772	0.624483	0.001403	0.02	0.642	0.358013	0.233934	5.73E-05

Drainage					Imbibition				
Rock Type 4 (RQI range from 0.5-1)					Rock Type 4 (RQI range from 0.5-1)				
P_c	S_l	S_g	K_{rl}	k_{rg}	P_c	S_l	S_g	K_{rl}	k_{rg}
1	0.736	0.264415	0.516846	0.004553	0.03	0.635	0.365222	0.224805	0.000156
1.5	0.530	0.469544	0.247276	0.046594	0.04	0.628	0.372245	0.216145	0.000315
2	0.424	0.575878	0.14486	0.106509	0.05	0.621	0.379087	0.207923	0.00054
3	0.314	0.685977	0.066547	0.216321	0.06	0.614	0.385757	0.200112	0.000837
4	0.257	0.74305	0.037386	0.298998	0.07	0.608	0.39226	0.192687	0.001205
5	0.222	0.778209	0.023425	0.360567	0.08	0.601	0.398603	0.185624	0.001648
6	0.198	0.802143	0.015709	0.40763	0.09	0.595	0.404792	0.178902	0.002165
7	0.180	0.819537	0.011027	0.444629	0.1	0.589	0.410832	0.172499	0.002755
8	0.167	0.832776	0.007996	0.474444	0.2	0.536	0.464129	0.122488	0.012366
9	0.157	0.843207	0.005936	0.498975	0.3	0.493	0.507166	0.090005	0.027205
10	0.148	0.851647	0.004484	0.519515	0.4	0.457	0.542681	0.067988	0.045221
12	0.136	0.864493	0.002649	0.551989	0.5	0.427	0.572511	0.05254	0.064908
14	0.126	0.873829	0.001606	0.576531	0.6	0.402	0.597939	0.041384	0.085264
18	0.113	0.886533	0.000591	0.611239	0.7	0.380	0.619885	0.033129	0.105653
20	0.109	0.891064	0.000345	0.623988	0.8	0.361	0.639028	0.026894	0.125682
25	0.101	0.899354	6.14E-05	0.647835	0.9	0.344	0.65588	0.022099	0.145117
30	0.095	0.904997	0	0.664456	1	0.329	0.670835	0.018353	0.163825
40	0.088	0.912	0	0.664456	2	0.238	0.76151	0.004223	0.308916
50	0.083	0.917	0	0.664456	3	0.195	0.804785	0.001439	0.398896
60	0.080	0.920	0	0.664456	4	0.170	0.830335	0.000595	0.458797
70	0.078	0.922	0	0.664456	5	0.153	0.847279	0.000275	0.501402
80	0.076	0.924	0	0.664456	6	0.141	0.859378	0.000136	0.533259
90	0.075	0.925	0	0.664456	7	0.132	0.86847	6.97E-05	0.557999
100	0.074	0.926	0	0.664456	8	0.124	0.875564	3.64E-05	0.577784
150	0.071	0.929	0	0.664456	9	0.119	0.881261	1.91E-05	0.593981
200	0.069	0.931	0	0.664456	10	0.114	0.885942	9.89E-06	0.607495
300	0.067	0.933	0	0.664456	12	0.107	0.893189	2.35E-06	0.628788
					14	0.101	0.898549	3.83E-07	0.64483
					20	0.091345	0.908655	0	0.664456
					30	0.082976	0.917024	0	0.664456
					40	0.078568	0.921432	0	0.664456
					50	0.075829	0.924171	0	0.664456
					60	0.073955	0.926045	0	0.664456

Imbibition				
Rock Type 4 (RQI range from 0.5-1)				
P_c	S_l	S_g	K_{rl}	k_{rg}
70	0.072588	0.927412	0	0.664456
80	0.071544	0.928456	0	0.664456
90	0.07072	0.92928	0	0.664456
100	0.070052	0.929948	0	0.664456
150	0.067993	0.932007	0	0.664456
200	0.066922	0.933078	0	0.664456
300	0.06581	0.93419	0	0.664456

Drainage					Imbibition				
Rock Type 5 (RQI range from 0.4-0.5)					Rock Type 5 (RQI range from 0.4-0.5)				
P_c	S_l	S_g	K_{rl}	k_{rg}	P_c	S_l	S_g	K_{rl}	k_{rg}
0	1.000	0	1	0	0	0.662	0.3376	0.303762	0
1.5	0.869	0.13133	0.728436	0.000433	0.005	0.660	0.340035	0.299527	9.31E-07
2	0.691	0.309055	0.426733	0.012203	0.01	0.658	0.342056	0.296043	4.32E-06
3	0.507	0.493071	0.196037	0.075452	0.02	0.654	0.346051	0.289234	2.17E-05
4	0.412	0.588461	0.110132	0.150391	0.03	0.650	0.349988	0.282627	5.66E-05
5	0.353	0.647226	0.069006	0.217992	0.04	0.646	0.353867	0.276216	0.000112
6	0.313	0.687229	0.046276	0.275433	0.05	0.642	0.35769	0.269993	0.00019
7	0.284	0.7163	0.032485	0.323737	0.06	0.639	0.361458	0.263952	0.000293
8	0.262	0.738428	0.023554	0.364521	0.07	0.635	0.365173	0.258086	0.000421
9	0.244	0.755861	0.017485	0.399251	0.08	0.631	0.368835	0.252388	0.000575
10	0.230	0.769968	0.013208	0.429108	0.09	0.628	0.372445	0.246854	0.000757
12	0.209	0.791439	0.007804	0.477694	0.1	0.624	0.376005	0.241476	0.000965
14	0.193	0.807042	0.004731	0.515487	0.2	0.591	0.409058	0.195229	0.004565
18	0.172	0.828276	0.00174	0.570433	0.3	0.562	0.43808	0.159845	0.010708
20	0.164	0.835848	0.001017	0.591042	0.4	0.536	0.463776	0.13233	0.018927
25	0.150	0.849704	0.000181	0.630181	0.5	0.513	0.486696	0.110624	0.028732
30	0.141	0.859136	0	0.657904	0.6	0.493	0.507273	0.093283	0.039698
40	0.129	0.871	0	0.657904	0.7	0.474	0.525854	0.079272	0.051479
50	0.121	0.879	0	0.657904	0.8	0.457	0.542719	0.067836	0.063798
60	0.116	0.884	0	0.657904	0.9	0.442	0.558101	0.058416	0.076443
70	0.113	0.887	0	0.657904	1	0.428	0.572188	0.050593	0.089247
80	0.110	0.890	0	0.657904	2	0.333	0.667435	0.015085	0.209236
90	0.108	0.892	0	0.657904	3	0.280	0.719672	0.005809	0.302188
100	0.106	0.894	0	0.657904	4	0.247	0.752861	0.00257	0.37216
150	0.100	0.900	0	0.657904	5	0.224	0.775901	0.001235	0.425955

Drainage					Imbibition				
Rock Type 5 (RQI range from 0.4-0.5)					Rock Type 5 (RQI range from 0.4-0.5)				
P_c	S_l	S_g	K_{rl}	k_{rg}	P_c	S_l	S_g	K_{rl}	k_{rg}
200	0.097	0.903	0	0.657904	6	0.207	0.792873	0.000623	0.468401
300	0.095	0.905	0	0.657904	7	0.194	0.805921	0.000323	0.50269
					8	0.184	0.816279	0.000169	0.530952
					9	0.175	0.824712	8.73E-05	0.554649
					10	0.168	0.831717	4.41E-05	0.574807
					12	0.157	0.842699	9.51E-06	0.607283
					14	0.149	0.85093	1.18E-06	0.632329
					20	0.133303	0.866697	0	0.657904
					30	0.119999	0.880001	0	0.657904
					40	0.112904	0.887096	0	0.657904
					50	0.108465	0.891535	0	0.657904
					60	0.105413	0.894587	0	0.657904
					70	0.103181	0.896819	0	0.657904
					80	0.101474	0.898526	0	0.657904
					90	0.100123	0.899877	0	0.657904
					100	0.099027	0.900973	0	0.657904
					150	0.095639	0.904361	0	0.657904
					200	0.093872	0.906128	0	0.657904
					300	0.092035	0.907965	0	0.657904

Drainage					Imbibition				
Rock Type 6 (RQI range from 0.3-0.4)					Rock Type 6 (RQI range from 0.3-0.4)				
P_c	S_l	S_g	K_{rl}	k_{rg}	P_c	S_l	S_g	K_{rl}	k_{rg}
0	1.000	0	1	0	0	0.666	0.3336	0.331434	0
2	0.877	0.123328	0.735111	0.000517	0.005	0.665	0.335485	0.327663	1.02E-06
3	0.641	0.359319	0.337702	0.028507	0.01	0.663	0.336962	0.324729	4.09E-06
4	0.518	0.481652	0.189719	0.085537	0.02	0.660	0.339892	0.31896	1.84E-05
5	0.443	0.557015	0.118874	0.147538	0.03	0.657	0.342789	0.313323	4.57E-05
6	0.392	0.608316	0.079717	0.205299	0.04	0.654	0.345654	0.307814	8.77E-05
7	0.354	0.645598	0.05596	0.256603	0.05	0.652	0.348489	0.302428	0.000146
8	0.326	0.673976	0.040575	0.301522	0.06	0.649	0.351293	0.297162	0.00022
9	0.304	0.696334	0.030121	0.340775	0.07	0.646	0.354066	0.292014	0.000313
10	0.286	0.714425	0.022753	0.375181	0.08	0.643	0.35681	0.286979	0.000423
12	0.258	0.74196	0.013444	0.432345	0.09	0.640	0.359525	0.282055	0.000551
14	0.238	0.761971	0.008151	0.477718	0.1	0.638	0.362211	0.277239	0.000699
18	0.211	0.789202	0.002998	0.544952	0.2	0.612	0.387591	0.234413	0.003207
20	0.201	0.798912	0.001751	0.570525	0.3	0.589	0.410551	0.199686	0.007508

Drainage					Imbibition				
Rock Type 6 (RQI range from 0.3-0.4)					Rock Type 6 (RQI range from 0.3-0.4)				
P_c	S_l	S_g	K_{rl}	k_{rg}	P_c	S_l	S_g	K_{rl}	k_{rg}
25	0.183	0.816682	0.000312	0.619585	0.4	0.569	0.431428	0.171251	0.013357
30	0.171	0.828778	0	0.654704	0.5	0.550	0.450496	0.147761	0.02048
40	0.156	0.844	0	0.654704	0.6	0.532	0.467985	0.1282	0.028619
50	0.146	0.854	0	0.654704	0.7	0.516	0.484086	0.111791	0.037549
60	0.140	0.860	0	0.654704	0.8	0.501	0.49896	0.097935	0.047081
70	0.135	0.865	0	0.654704	0.9	0.487	0.512744	0.086162	0.057056
80	0.131	0.869	0	0.654704	1	0.474	0.525556	0.076101	0.067344
90	0.129	0.871	0	0.654704	2	0.383	0.617117	0.025884	0.171715
100	0.126	0.874	0	0.654704	3	0.329	0.671216	0.010677	0.261114
150	0.119	0.881	0	0.654704	4	0.293	0.70711	0.004916	0.332769
200	0.116	0.884	0	0.654704	5	0.267	0.732746	0.002417	0.390243
300	0.112	0.888	0	0.654704	6	0.248	0.752016	0.001235	0.436996
					7	0.233	0.767054	0.000642	0.475643
					8	0.221	0.779132	0.000334	0.508076
					9	0.211	0.789057	0.000171	0.535663
					10	0.203	0.797364	8.46E-05	0.55941
					12	0.189	0.810502	1.67E-05	0.598202
					14	0.180	0.82044	1.58E-06	0.628559
					20	0.160303	0.839697	0	0.654704
					30	0.143833	0.856167	0	0.654704
					40	0.134967	0.865033	0	0.654704
					50	0.129393	0.870607	0	0.654704
					60	0.125548	0.874452	0	0.654704
					70	0.122729	0.877271	0	0.654704
					80	0.12057	0.87943	0	0.654704
					90	0.118859	0.881141	0	0.654704
					100	0.11747	0.88253	0	0.654704
					150	0.113167	0.886833	0	0.654704
					200	0.110919	0.889081	0	0.654704
					300	0.108578	0.891422	0	0.654704

Drainage					Imbibition				
Rock Type 7 (RQI range from 0.2-0.3)					Rock Type 7 (RQI range from 0.2-0.3)				
P_c	S_l	P_c	S_l	P_c	S_l	P_c	S_l	P_c	S_l
0	1.000	0	1	0	0	0.675	0.325	0.373628	0
3	0.874	0.126025	0.713363	0.00093	0.005	0.674	0.325972	0.371226	1.32E-07
4	0.704	0.295794	0.400764	0.020055	0.01	0.673	0.32694	0.368843	1.34E-06
5	0.600	0.400378	0.251109	0.059641	0.02	0.671	0.328866	0.364134	8.78E-06
6	0.528	0.471572	0.168394	0.107504	0.03	0.669	0.330777	0.3595	2.42E-05

Drainage					Imbibition				
Rock Type 7 (RQI range from 0.2-0.3)					Rock Type 7 (RQI range from 0.2-0.3)				
P_c	S_l	P_c	S_l	P_c	S_l	P_c	S_l	P_c	S_l
7	0.477	0.523311	0.11821	0.156382	0.04	0.667	0.332674	0.354939	4.86E-05
8	0.437	0.562692	0.08571	0.203061	0.05	0.665	0.334557	0.350451	8.25E-05
9	0.406	0.593719	0.063627	0.246344	0.06	0.664	0.336427	0.346033	0.000127
10	0.381	0.618825	0.048063	0.285955	0.07	0.662	0.338282	0.341684	0.000181
12	0.343	0.657037	0.028399	0.354793	0.08	0.660	0.340124	0.337403	0.000246
14	0.315	0.684807	0.017217	0.41181	0.09	0.658	0.341953	0.333189	0.000323
18	0.277	0.722597	0.006334	0.499664	0.1	0.656	0.343769	0.32904	0.00041
20	0.264	0.736073	0.003699	0.534031	0.2	0.639	0.361226	0.290889	0.001907
25	0.239	0.760732	0.000658	0.601293	0.3	0.622	0.377506	0.258077	0.004516
30	0.222	0.777518	0	0.650445	0.4	0.607	0.392727	0.229724	0.008143
40	0.201	0.799	0	0.650445	0.5	0.593	0.406991	0.205113	0.012669
50	0.188	0.812	0	0.650445	0.6	0.580	0.420385	0.183663	0.017973
60	0.179	0.821	0	0.650445	0.7	0.567	0.43299	0.164895	0.023938
70	0.172	0.828	0	0.650445	0.8	0.555	0.444872	0.148415	0.030462
80	0.167	0.833	0	0.650445	0.9	0.544	0.456095	0.133894	0.03745
90	0.163	0.837	0	0.650445	1	0.533	0.466712	0.12106	0.04482
100	0.160	0.840	0	0.650445	2	0.452	0.548164	0.048647	0.127684
150	0.150	0.850	0	0.650445	3	0.399	0.601328	0.022053	0.208901
200	0.145	0.855	0	0.650445	4	0.361	0.638888	0.010743	0.280171
300	0.140	0.860	0	0.650445	5	0.333	0.666901	0.005458	0.341131
					6	0.311	0.688635	0.002831	0.393146
					7	0.294	0.706012	0.001474	0.437759
					8	0.280	0.720239	0.000758	0.476313
					9	0.268	0.732112	0.000377	0.509902
					10	0.258	0.742177	0.000178	0.539395
					12	0.242	0.758338	2.85E-05	0.588718
					14	0.229	0.77076	1.24E-06	0.628299
					20	0.20468	0.79532	0	0.650445
					30	0.18316	0.81684	0	0.650445
					40	0.171379	0.828621	0	0.650445
					50	0.163902	0.836098	0	0.650445
					60	0.158714	0.841286	0	0.650445

Imbibition				
Rock Type 7 (RQI range from 0.2-0.3)				
S_l	P_c	S_l	P_c	S_l
70	0.154895	0.845105	0	0.650445
80	0.15196	0.84804	0	0.650445
90	0.14963	0.85037	0	0.650445
100	0.147734	0.852266	0	0.650445
150	0.141841	0.858159	0	0.650445
200	0.13875	0.86125	0	0.650445
300	0.135525	0.864475	0	0.650445

Drainage					Imbibition				
Rock Type 8 (RQI range from 0.1-0.2)					Rock Type 8 (RQI range from 0.1-0.2)				
P_c	S_l	P_c	S_l	P_c	S_l	P_c	S_l	P_c	S_l
0	1.000	0	1	0	0	0.698	0.3025	0.445231	0
5	0.941	0.059018	0.838383	0.000148	0.005	0.696	0.303506	0.441579	1.36E-06
6	0.826	0.174245	0.56222	0.006198	0.01	0.696	0.304011	0.439754	3.44E-06
7	0.742	0.257984	0.394669	0.024002	0.02	0.695	0.305017	0.43613	1.08E-05
8	0.678	0.321723	0.286162	0.051411	0.03	0.694	0.30602	0.43254	2.28E-05
9	0.628	0.37194	0.212433	0.084796	0.04	0.693	0.307018	0.428985	3.98E-05
10	0.587	0.412576	0.160468	0.121264	0.05	0.692	0.308013	0.425464	6.18E-05
12	0.526	0.474422	0.094815	0.196341	0.06	0.691	0.309003	0.421976	8.91E-05
14	0.481	0.519367	0.057484	0.268306	0.07	0.690	0.309989	0.418521	0.000122
18	0.419	0.580531	0.021146	0.393949	0.08	0.689	0.310971	0.4151	0.00016
20	0.398	0.602342	0.012351	0.447404	0.09	0.688	0.31195	0.41171	0.000204
25	0.358	0.642253	0.002198	0.55825	0.1	0.687	0.312924	0.408353	0.000253
30	0.331	0.669422	0	0.64403	0.2	0.678	0.322455	0.376468	0.00106
40	0.296	0.704	0	0.64403	0.3	0.668	0.331617	0.347426	0.002437
50	0.274	0.726	0	0.64403	0.4	0.660	0.340431	0.320934	0.004363
60	0.260	0.740	0	0.64403	0.5	0.651	0.348917	0.296735	0.006805
70	0.249	0.751	0	0.64403	0.6	0.643	0.357093	0.274601	0.009727
80	0.241	0.759	0	0.64403	0.7	0.635	0.364976	0.254329	0.013089
90	0.235	0.765	0	0.64403	0.8	0.627	0.372581	0.23574	0.016856
100	0.230	0.770	0	0.64403	0.9	0.620	0.379925	0.218674	0.020989
150	0.214	0.786	0	0.64403	1	0.613	0.387019	0.202989	0.025457
200	0.206	0.794	0	0.64403	2	0.553	0.446681	0.099601	0.082468
300	0.197	0.803	0	0.64403	3	0.509	0.491341	0.0509	0.149335
					4	0.474	0.526085	0.026542	0.216548
					5	0.446	0.553924	0.013886	0.280345
					6	0.423	0.576754	0.007172	0.339428

Imbibition				
Rock Type 8 (RQI range from 0.1-0.2)				
S_l	P_c	S_l	P_c	S_l
7	0.404	0.595832	0.003592	0.393561
8	0.388	0.612026	0.001704	0.442954
9	0.374	0.625951	0.00074	0.487988
10	0.362	0.638059	0.000278	0.529089
12	0.342	0.658102	1.31E-05	0.601124
14	0.325968	0.674032	0	0.64403
20	0.293082	0.706918	0	0.64403
30	0.262675	0.737325	0	0.64403
40	0.245378	0.754622	0	0.64403
50	0.234156	0.765844	0	0.64403
60	0.226259	0.773741	0	0.64403
70	0.220385	0.779615	0	0.64403
80	0.215838	0.784162	0	0.64403
90	0.212208	0.787792	0	0.64403
100	0.20924	0.79076	0	0.64403
150	0.19994	0.80006	0	0.64403
200	0.195016	0.804984	0	0.64403
300	0.189845	0.810155	0	0.64403

Drainage					Imbibition				
Rock Type 9 (RQI range from 0.01-0.1)					Rock Type 9 (RQI range from 0.01-0.1)				
P_c	S_l	P_c	S_l	P_c	S_l	P_c	S_l	P_c	S_l
0	1.000	0	1	0	0	0.831	0.1688	0.631603	0
18	0.900	0.099708	0.471353	0.015556	0.005	0.831	0.169147	0.626831	1.73E-06
20	0.850	0.150401	0.275312	0.060399	0.01	0.831	0.169294	0.624815	3.93E-06
25	0.757	0.243167	0.048989	0.294839	0.02	0.830	0.169588	0.620801	1.12E-05
30	0.694	0.306314	0	0.631616	0.03	0.830	0.169882	0.616809	2.24E-05
40	0.613	0.387	0	0.631616	0.04	0.830	0.170175	0.61284	3.76E-05
50	0.563	0.437	0	0.631616	0.05	0.830	0.170468	0.608892	5.7E-05
60	0.529	0.471	0	0.631616	0.06	0.829	0.170761	0.604966	8.06E-05
70	0.505	0.495	0	0.631616	0.07	0.829	0.171053	0.601063	0.000108
80	0.486	0.514	0	0.631616	0.08	0.829	0.171345	0.59718	0.000141
90	0.471	0.529	0	0.631616	0.09	0.828	0.171636	0.59332	0.000177
100	0.459	0.541	0	0.631616	0.1	0.828	0.171928	0.589481	0.000218
150	0.422	0.578	0	0.631616	0.2	0.825	0.174819	0.552249	0.000874
200	0.403	0.597	0	0.631616	0.3	0.822	0.177674	0.517051	0.001983
300	0.384	0.616	0	0.631616	0.4	0.820	0.180494	0.483787	0.003547
					0.5	0.817	0.183279	0.452362	0.005563

Imbibition				
Rock Type 9 (RQI range from 0.01-0.1)				
S_l	P_c	S_l	P_c	S_l
0.6	0.814	0.186031	0.422686	0.008024
0.7	0.811	0.188749	0.394671	0.010921
0.8	0.809	0.191435	0.368237	0.014245
0.9	0.806	0.194089	0.343304	0.017986
1	0.803	0.196711	0.319798	0.022133
2	0.779	0.221319	0.149136	0.083595
3	0.757	0.243326	0.060698	0.174405
4	0.737	0.26313	0.019561	0.286135
5	0.719	0.28105	0.003917	0.41234
6	0.703	0.297347	0.000175	0.548192
7	0.687765	0.312235	0	0.631616
8	0.674108	0.325892	0	0.631616
9	0.661533	0.338467	0	0.631616
10	0.649915	0.350085	0	0.631616
12	0.629135	0.370865	0	0.631616
14	0.611084	0.388916	0	0.631616
20	0.568761	0.431239	0	0.631616
30	0.522277	0.477723	0	0.631616
40	0.491998	0.508002	0	0.631616
50	0.470635	0.529365	0	0.631616
60	0.454717	0.545283	0	0.631616
70	0.442376	0.557624	0	0.631616
80	0.432514	0.567486	0	0.631616
90	0.424443	0.575557	0	0.631616
100	0.41771	0.58229	0	0.631616
150	0.395809	0.604191	0	0.631616
200	0.383707	0.616293	0	0.631616
300	0.370611	0.629389	0	0.631616